The SWOT Mission and Its Capabilities for Land Hydrology

Sylvain Biancamaria, Dennis Lettenmaier, Tamlin Pavelsky

The SWOT mission and capabilities for land hydrology

Sylvain Biancamaria
CNRS, LEGOS, UMR5566 CNRS-CNES-IRD-Université de Toulouse III
14 avenue Edouard Belin
31400 Toulouse
France
Email: sylvain.biancamaria@legos.obs-mip.fr
Tel.: +335.61.33.29.15
Fax: +335.67.04.40.14

Dennis P Lettenmaier
University of California - Los Angeles
Department of geography
1145 Bunche Hall
Los Angeles, CA 90095-1524

Tamlin M Pavelsky
University of North Carolina
Department of Geological Sciences
104 South Rd. CB #3315
Chapel Hill, NC 27599-3315

Published in Surveys in Geophysics (2016), doi:10.1007/s10712-015-9346-y

Abstract

Surface water storage and fluxes in rivers, lakes, reservoirs and wetlands are currently poorly observed at the global scale, even though they represent major components of the water cycle and deeply impact human societies. *In situ* networks are heterogeneously distributed in space, and many river basins and most lakes – especially in the developing world and in sparsely populated regions – remain unmonitored. Satellite remote sensing has provided useful complementary observations, but no past or current satellite mission has yet been specifically designed to observe, at the global scale, surface water storage change and fluxes. This is the purpose of the planned Surface Water and Ocean Topography (SWOT) satellite mission. SWOT is a collaboration among the (U.S.) National Aeronautics and Space Administration (NASA), Centre National d'Études Spatiales (CNES, the French Spatial Agency), the Canadian Space Agency (CSA), and the United-Kingdom Space Agency (UKSA), with launch planned in late 2020. SWOT is both a continental hydrology and oceanography mission. However, only the hydrology capabilities of SWOT are discussed here. After a description of the SWOT mission requirements and measurement capabilities, we review the SWOT-related studies concerning land hydrology published to date. Beginning in 2007, studies demonstrated the benefits of SWOT data for river hydrology, both through discharge estimation directly from SWOT measurements and through assimilation of SWOT data into hydrodynamic and hydrology models. A smaller number of studies have also addressed methods for computation of lake and reservoir storage change or have quantified improvements expected from SWOT compared to current knowledge of lake water storage variability. We also briefly review other land hydrology capabilities of SWOT, including those related to transboundary river basins, human water withdrawals, and wetland environments. Finally, we discuss additional studies needed before and after the launch of the mission, along with perspectives on a potential successor to SWOT.

Keywords: Surface Water and Ocean Topography (SWOT) satellite mission; continental surface waters; lakes; reservoirs; rivers

1. SWOT mission overview

1.1. The needs for a global water surface mission and its requirements

In the late 1990s and early 2000s, the crucial need for more quantitative data on spatiotemporal dynamics of surface waters at a global scale became clear in context of a declining *in situ* gage network and increasing need to observe and model the global water cycle (Alsdorf et al. 2003). To address this challenge, Alsdorf and Lettenmaier (2003) advocated development of a "topographic imager" satellite mission with ~100 m spatial resolution (to observe main channels, floodplains and lakes), temporal resolution on the order of a few days (to sample flood waves and river dynamic at basin scale), and capability to measure height changes that characterize variations in river discharge and lake water storage. Alsdorf et al. (2007) provided a more in-depth study showing that "spatial and temporal dynamics of surface freshwater discharge and changes in storage globally" are poorly known because:

- *in situ* networks are very heterogeneous (some countries have dense networks, whereas others have a few measurements points),
- these data are not always shared at the international level,
- current satellite missions do not provide measurements adequate to observe global spatio-temporal dynamics of continental water surface.

For that reason, Alsdorf et al. (2007) proposed a new satellite mission based on synthetic aperture radar (SAR) interferometry, called Water and Terrestrial Elevation Recovery (WATER). The concept of this satellite mission is built on the legacy of the Shuttle Radar Topography Mission (SRTM) and the Wide Swath Ocean Altimeter (WSOA). SRTM (Farr et al. 2007) was a SAR interferometer in C- and X-bands that flew in February 2000 on the NASA Space Shuttle Endeavour. SRTM provided a near-global Digital Elevation Model (DEM) at 90 m spatial resolution between 60°S and 60°N, but because of the specular returns characteristic of its oblique look angles (between 30° and 60°) it provided poor measurements of surface water. Because the two interferometric antennas were separated by a 60 m mast, construction of an SRTM-like system on a satellite platform would be problematic. A similar concept, WSOA, was envisioned as an additional payload to the altimetry Jason-2 satellite mission with the aim of imaging ocean topography. The distance between the two Ku-band antennas was set to 6.4 m to facilitate inclusion on a satellite platform (resulting in kilometric pixel resolution), and a near-nadir look angle was chosen to better observe the ocean surface (Fu and Rodríguez 2004). WSOA was definitely withdrawn in 2004 and never flown. To adapt this concept to the needs of continental water surface observation, Alsdorf et al. (2007) proposed to use Ka-band instead of Ku-band, allowing better

spatial resolution (see section 1.2). In 2007, in its Decadal Survey (NRC 2007), the National Research Council recommended to NASA this new satellite mission, under the name Surface Water and Ocean Topography (SWOT, https://swot.jpl.nasa.gov/), to measure both the ocean and land water surface topography. Since then, SWOT has been collaboratively developed by NASA, the Centre National d'Etudes Spatiales (CNES, the French space agency) and more recently the Canadian Space Agency (CSA/ASC) and the United-Kingdom Space Agency (UKSA). Currently, SWOT is planned for launch in late 2020. It will observe the whole continental waters-estuaries-ocean continuum and therefore link the ocean and hydrology scientific communities. However, in this paper, the ocean component of the mission will not be addressed.

Figure 1 gives an overview of the main spatiotemporal physical processes related to the land hydrological cycle and the SWOT observation window. SWOT is designed to observe a large fraction of rivers and lakes globally and will provide robust observations of their seasonal cycles. However, at least by itself, it is not conceived to observe climate-scale variability (and especially climate change) and will not be able (except on rare occasions) to monitor flash floods. As stated by Rodríguez (2015), SWOT aims to address the following hydrologic science questions:

- What are the temporal and spatial scales of the hydrologic processes controlling surface water storage and transport across the world's continents?
- What are the spatially distributed impacts of humans on surface water, for example through water impoundment behind dams, withdrawals and releases to rivers and lakes, trans-boundary water sharing agreements, diversions, levees, and other structures?
- What are the regional- to global-scale sensitivities of surface water storages and transport to climate, antecedent floodplain conditions, land cover, extreme droughts, and the cryosphere?
- Can regional and global extents of floodable land be quantified through combining remotely sensed river surface heights, widths, slopes, and inundation edge with coordinated flood modeling?
- What are the hydraulic geometries and three-dimensional spatial structures of rivers globally, knowledge of which will improve our understanding of water flow?

The scientific rationales for these questions and the measurement needs are presented in the SWOT Mission Science Document (Fu et al. 2012). Based on these needs, the SWOT Science Requirements (Rodríguez 2015, summed up in Table 1) have been derived to design the SWOT mission, which is presented in subsections 1.2 to 1.4 (sections 1.2 for the main payload, section 1.3 concerning SWOT products over land and section 1.4 for its spatiotemporal sampling). Then, sections 2 and 3 present the benefits of SWOT for measurement of rivers and other water bodies, respectively.

1.2. Characteristics of the KaRIn instrument

To meet the SWOT science requirements (Table 1), a Ka-band Radar Interferometer (KaRIn) has been designed as the mission main payload. KaRIn will be a SAR interferometer in Ka-band (35.75 GHz frequency or 8.6 mm wavelength), with near nadir incidence angles (between 0.6° and 3.9°, Fjørtoft et al. 2014). Figure 2 shows a conceptual view of the KaRIn operating system and ground coverage. It will provide images of water elevations within two swaths, one on each side of the satellite. These two swaths (each 50 km wide) will be separated by a 20 km gap at the satellite nadir (Figure 2). KaRIn will operate in bistatic mode: one antenna emits the electromagnetic signal towards the closest swath and the two antennas (10 m apart) receive the backscattered signal in their respective directions. Interferometry effectively involves a triangulation: each point in the swath will be observed from two different positions (the antennas positions), which will allow precise estimation of the location of each point. More precisely, the phase difference between the backscattered signals received by the two antennas (the so-called interferogram) will be used to invert water elevations. More details of SAR interferometry and the KaRIn measurements are provided in chapters 6 and 7 in Fu et al. (2012) and by Fjørtoft et al. (2014). Table 2 summarizes the main characteristics of the KaRIn instrument.

KaRIn will provide images of water surface elevation with pixel sizes ~6 m in the azimuth direction (direction of the satellite orbit) and from 60 m (near range, see Fig. 2) to 10 m (far range) in the range direction (perpendicular to the azimuth), as also indicated in Table 2 (Fu et al., 2012, Fjørtoft et al. 2014, Biancamaria et al. 2010). However, it should be clearly understood that this image is obtained in “radar projection” and not in a geolocated projection. Indeed, the radar instrument measures the distance between the observed point and the antenna. Therefore, in radar images, two consecutive pixels in the range direction correspond to points on the ground that have a similar distance from the satellite. For that reason, when pixels are geolocated they are more scattered, they do not correspond to a regular grid, and their shape becomes distorted. For example, a hill, which is few km away from a river, could have a distance to the satellite similar to that of the center of the river and therefore could be located close to the river center in a SAR image. However, in this example, the river banks will have a different distance from the satellite and could be several pixels distant from the river center pixel. Therefore, the top of the hill will be closer to the river center than the river banks. This effect, hereafter referred to as “layover”, occurs when surrounding topography or vegetation is at the same distance from the satellite as the water surface (land over water layover). Furthermore, pixels with large vertical errors will also have high geolocation error (vertical and horizontal accuracies are functions of the phase interferogram accuracy). For that reason, the most basic geolocated SWOT products will likely be delivered as point cloud products that can more accurately take into account these geolocation inversion effects (Rodríguez 2015).

The 10 m to 60 m x 6 m intrinsic pixel size also can be somewhat misleading, as a SWOT measurement requirement (Table 2) is not given for this spatial resolution. While these pixels represent the basic unit of SWOT measurement, in fact, water elevations measured by the KaRIn instrument at this native pixel size will be metric if not decametric in accuracy. Achieving the decimetric accuracy that is a stated requirement in Rodríguez (2015) and Table 2 will require averaging over many such pixels. This issue is discussed in more detail in the section 1.3.

In Ka-band, water is more or less specular, whereas land is rougher. KaRIn near-nadir incidence angles are particularly suited to monitor water bodies, as water will backscatter most of the emitted energy toward the satellite nadir (because of its specular behavior and the near-nadir look angle), whereas land will backscatter energy in all directions and therefore less in the antenna direction. Because of this different energy scattering between water and land, the difference in amplitude of the received electromagnetic wave between water and non-water pixels should be quite high and will be used to compute the water mask. However, because SWOT look angles are close to the nadir, but not exactly at the nadir, some water surface roughness is still needed to get sufficient energy. Thus, when the water surface becomes extremely flat, typically for wind speed $<< 1$ m.s^{-1}, there could be some loss of data in the far-swath where look angle are close to 3.9° (Enjolras and Rodríguez 2009, Moller and Esteban-Fernandez 2015). This issue is currently under investigation using measurements from the AirSWOT platform, an airborne SWOT analogue (Rodriguez et al. 2010), obtained during campaigns conducted in 2014 and 2015. It will allow better quantification of the frequency and magnitude of layover effects.

Very few satellite missions have used Ka-band, which is therefore not as well understood as lower frequency bands. For example, most current nadir altimeters use Ku- or C-bands, whereas SAR imaging missions are in L-, C- or X-bands. Additionally, these current sensors have lower (nadir altimeters) or higher (SAR imagery missions) observation incidence angles than SWOT. However, using Ka-band instead of higher wavelength bands has several advantages: first, it allows a finer spatial resolution (which is dependent on the electromagnetic wavelength) from the SAR processing and second, it facilitates a shorter baseline (distance between the two antennas) for a given targeted instrumental vertical accuracy, for the interferometry processing (a shorter baseline corresponds to a shorter mast between the two antennas, which is easier to construct). Shorter wavelengths also result in less penetration into soil, snow and vegetation (Fjørtoft et al. 2014), which should allow better estimation of wetland and saturated soil surface elevation and snow volume variations, if interferograms can be computed.

A drawback of Ka-band is its sensitivity to rain rates above about 3 mm/hour (Rodríguez 2015). The only altimetry satellite mission in Ka-band preceding SWOT is the Satellite with Argos and ALtiKa (SARAL) mission with the AltiKa nadir altimeter, launched only recently (February 2013).

Measurements obtained from this new instrument will help to better understand backscattering in Ka-band over different surfaces (water, bare soil, vegetation, snow, etc). However, AltiKa, as a nadir altimeter, does not have exactly SWOT look angles; its measurements integrate all the energy backscattered in a cone covering angles between -0.3° and 0.3° to the nadir (AltiKa half antenna aperture is 0.3°, Steunou et al. 2015). The Global Precipitation Measurement (GPM) Mission Core Observatory, launched in February 2014, carries the Dual-Frequency Precipitation Radar (DPR) in Ku and Ka bands (http://pmm.nasa.gov/GPM/flight-project/DPR). In Ka-band, DPR scans across a 125 km swath (±8.5° across track) with a 5 km footprint. Analyzing DPR measurements will provide useful information on backscatter properties in Ka-band, however the GPM observation angle covers a wider range than SWOT with a much coarser spatial resolution. For those reasons, airborne and field campaigns have been organized by the Jet Propulsion Laboratory (JPL) (Moller and Esteban-Fernandez 2015) and CNES (Fjørtoft et al. 2014) to better understand Ka-band backscattering at SWOT-like incidence angles. These campaigns have confirmed the decrease of the backscatter coefficient with the incidence angle and a water/land backscatter coefficient contrast of around 10 dB, except when the water surface is very flat (low wind speed and hence extremely low surface roughness). Moller and Esteban-Fernandez (2015) have also reported the impact of decorrelation time (and therefore wind speed and water surface turbulence) on pixel azimuth size, which could become higher than expected based on the instrument characteristics (Table 2). In addition to KaRIn, SWOT will carry additional scientific payload (Table 2), including a dual frequency (Ku and C-band) nadir altimeter, similar to the Poseidon-3 instrument on-board Jason-2 (Desjonquères et al. 2010). It will provide water elevation measurements in the middle of the 20 km gap between the two KaRIn swaths. A radiometer will also facilitate, over the oceans, corrections to path delay due to wet tropospheric effects. However, it will not be used over land because land emissivity dominates the radiometric signal (Fu et al. 2012). Wet troposphere corrections over land will be computed using an atmospheric model, one effect of which will be that the residual tropospheric error will likely be larger over land than over the ocean and should be on the order of 4 cm (Fu et al. 2012).

1.3 SWOT measurements over terrestrial surface waters

SWOT will provide measurements of surface water elevation, slope and water mask. **In this paper, water elevation (*H*) corresponds to the distance between the top of the water surface and a given reference surface (geoid or ellipsoid), whereas water depth (*d*) corresponds to the distance between the water surface and the water body (e.g. river) bottom**. It is important to note that SWOT will not measure water depth. SWOT level-2 data products (i.e. the highest level of

processed data delivered by NASA and CNES to end-users) are currently being defined. There remains, therefore, some uncertainty as to their specific nature. However, some characteristics of SWOT level-2 data product over land are provided in the science requirements document (Rodríguez 2015), which is the basis for the discussion in this section. As outlined in Rodríguez (2015) these products will likely include:

- For each pass, a water mask consisting of a geolocated point cloud product with all KaRIn pixels that are identified as water, with the finest spatial resolution to meet appropriate geolocation accuracy (i.e. 10% of the pixel size in any direction). Surface water elevation corresponding to the provided pixel size (with an estimation of the surface water elevation uncertainty) will be associated with each point within the water mask.
- At least once every repeat cycle, a global water mask following the shorelines of all observed water bodies will be provided in vector format, with one water elevation for each individual water body, along with other information (such as area within the water body and its slope). Water storage within each such water body will be easily derived from this product.
- A global one-dimensional vector product that will include estimated discharge along river reaches at each observation time, for all river reaches wider than 50 m.
- A cross-section map of all observed water bodies will be derived from time-varying water elevations along the shores of each water body. This map will be updated yearly.

As SWOT will observe almost all continental surfaces every 21 days, it will provide a tremendous amount of data in the point cloud product, which includes the KaRIn pixels resolution stated in Table 2 (as a reminder, vertical accuracy at such spatial resolution is very low). It will therefore be very difficult for end-users to use so much data in a non-gridded format at global, regional or even basin scales. For that reason, vector products providing height integrated measurements for entire lakes and for discrete river reaches have been defined.

The SWOT mission is designed to observe all rivers wider than 100 m and water bodies (lakes, reservoirs, ponds, continuous wetlands) with an area greater than 250 m x 250 m (i.e. 62 500 m^2) that lie within the swath coverage. Moreover, NASA and CNES teams will strive to design an instrument and processing methods that will be able to observe rivers wider than 50 m and water bodies with an area above 100 m x 100 m. If SWOT is able to observe smaller rivers or water bodies, the measured data will be provided. Besides, lower level product (SAR amplitude and phase images, interferograms) will be provided on-demand and could be used to reprocess data a posteriori, which might help to improve products resolution if feasible. The main sources of errors that will affect KaRIn measurements are instrument thermal noise (white noise), differences in the return signal speckle, error in the interferometric baseline roll angle, wet and dry tropospheric effects, ionospheric effects, topographic layover and vegetation layover and attenuation (see chapter

6 in Fu et al. 2012). Thermal noise and speckle dominates the error budget at the KaRIn pixel level (10 m to 60 m x 6 m, Table 2), leading to multi-meter vertical errors. These errors are random for one pixel, but their standard deviations tend to increase in the far range of the measurement swath (Enjolras and Rodríguez 2009). Fortunately, these random errors can be reduced by averaging over water pixels by the square root of the number of pixels averaged. For this reason, the science requirements (Table 1) are provided for water areas much larger than a single pixel. However, the other sources of error will not be reduced by the averaging process. Over 1 km^2 (e.g. a 10 km reach for a river of 100 m width), SWOT water elevation will have a 10 cm (1 σ) accuracy. For this averaging area, random errors and wet tropospheric effects are the main error sources. Locally, especially near the water bodies margins, topographic and vegetation layover can be a source of large errors, especially given the near nadir incidence angles used by KaRIn. Therefore, the received energy by the antenna will be a mixture of the energy backscattered by water and topography or vegetation, leading to potentially large errors in retrieved water elevation, geolocation and water extent. SWOT performance will be evaluated for water bodies meeting the observation requirement (lakes, reservoirs, and wetlands with area greater than 250 m x 250 m and rivers wider than 100 m), in order to validate that the instrument meets the accuracies provided in Table 1. Furthermore, SWOT performance will be characterized for the observational goals (100 m x 100 m to 250 m x 250 m water bodies and 50 m to 100 m wide rivers). Estimates of measurement accuracy will be provided with SWOT data products.

There is currently no near-real time consideration for provision of SWOT data products, consistent with the scientific rather than operational nature of the mission. However, derived products are expected to be provided within 60 days of their collection (requirement). There is also a goal to provide water elevations for a select number of reservoirs (less than 1000) within 30 days of collection. Finally, it is worth noting that an on-board averaged ocean water elevation product computed over a regular grid will also be provided over continents (all observed pixels will be available, not just the ones that are entirely covered by water). This ocean product will have a spatial resolution between 250 m and 1 km (the grid size has not yet been finalized). However, while the elevation accuracy over oceans will be centimetric, the accuracy of this product over continents is not defined and has not yet been evaluated, in part because SAR interferometry processing over land is much more complex than over oceans.

1.4. SWOT spatiotemporal coverage

There will be an initial calibration phase for the SWOT mission with a fast sampling orbit (1-day repeat period), but reduced spatial coverage relative to the subsequent orbit. The objective of this

fast sampling phase of the mission is to obtain frequent overpasses of the satellite over specific ocean/land hydrology targets that will allow calibration of radar system parameters. For open oceans, it will also help to characterize water elevation temporal decorrelation times. This initial calibration phase will last three months, which is expected to be sufficient to obtain a fully calibrated system for the nominal phase (Rodríguez 2015). The nominal phase of the mission (also termed the science phase), will have a non-sun synchronous, 890.5 km altitude, 20.86 day repeat period and 77.6° inclination orbit (Table 2) and will last at least 3 years. The remainder of this section is applicable only to this nominal orbit.

SWOT spatial coverage and revisit times per orbit repeat period (i.e. ~21 days) depend on orbit characteristics, instrument swath width (2x50 km), nadir gap width (20 km) and is a function of latitude as well. Figure 3 shows a map of the number of SWOT revisits per orbit repeat period (~21 days) over the continents between 78°S and 78°N (a.). To improve figure readability and given the scope of this paper, oceans have been masked in blue. However, oceans and continents will have the same sampling pattern. Figure 3.b shows the Lower Amazon basin, which illustrates the extent of locations that will never be sampled by SWOT (white diamonds). Tropical regions will be sampled less frequently than higher latitudes; the number of revisits per repeat period ranges from a maximum of two at the equator to more than ten above 70°N/S. Few regions will never be observed (white in Figures 3.a and 3.b); however much of the equatorial regions will be seen only once per repeat period.

Figure 3 also shows that the mission will observe almost all continental surfaces from 78°S to 78°N, which will be a tremendous improvement compared to nadir altimeters, which miss many water bodies. Regions not observed by SWOT are the results of the 20 km nadir gap between the two swaths (white diamonds without magenta boundaries on Figure 3.b) and the orbit intertrack distance, which does not always allow for adjacent swaths to overlap at the lowest latitudes (white diamonds with magenta boundaries on Figure 3.b). Gaps due to orbit intertrack distance are only present in the 25°S-25°N latitude band, with their largest extent between 10°S and 10°N. Coverage gaps resulting from the nadir gap cover a much broader latitude band (60°S-60°N) and are the main source of observation gaps. The total gap area over all latitudes between 78°S and 78°N is about 3.55% of the whole land area (or 4.90×10^6 km^2). This is consistent with the SWOT science requirement (Rodríguez 2015), which states: “SWOT shall collect data over a minimum of 90% of all ocean and land areas covered by the orbit inclination for 90% of the operation time” (Table 2). The coverage gap can, however, be locally higher than 10% between 10°S and 10°N. On average over this band of latitudes, 7% of land is unobserved and the maximum coverage gap is 14% over a 1° latitude band centered on 4.5°N.

Satellite nadir altimeters measure water elevation along the satellite tracks, and therefore, most

sampled river reaches are observed only once per repeat period (except for the few locations where ascending and descending tracks cross). Thus, temporal sampling of rivers by nadir altimeters is essentially equal to the orbit repeat period. Large lakes may be sampled more than once during a repeat cycle by altimeters, but uncertainties in the geoid when different parts of a lake are sampled must be corrected for (Crétaux et al., 2011). These difficulties will be overcome for SWOT, as for most locations in both rivers and lakes there will be more than one observation per repeat period for the reasons indicated above. The number of revisits is, however, unevenly distributed in time during the repeat period. This is illustrated in Figure 4, which shows the SWOT observation mask (black bars correspond to observation dates) for all latitudes along the 30°E meridian versus days during a repeat period. For example, at the equator and at 30°E, there will be two observations: one at day 15 and one at day 20, but no observations for 16 consecutive days. The distribution of revisit times during a repeat period does not monotonically controlled by latitude, which makes it difficult to infer directly how errors from temporal sampling vary as a function of latitude. SWOT products that will be used for seasonal studies may require computing monthly time series. The uneven SWOT temporal sampling will be a source of error in the computation of monthly means. Computing cycle-based averaged (i.e. 21-days average) might be a viable alternative for SWOT, but this option requires additional study. The impacts of these variations in temporal sampling depend on the nature of the water body sampled. For example, the water surface elevation of some lakes may not vary significantly except on monthly or longer timescales, while many rivers exhibit changes in discharge on daily or even hourly timescales. In rivers, errors associated with gaps in temporal sampling result from missed local maximum/minimum flows (Biancamaria et al. 2010, Papa et al. 2012), the importance of which depends on the flashiness of the river. To estimate error in monthly averages due only to the SWOT uneven temporal sampling, Biancamaria et al. (2010) proposed a method that used daily *in situ* discharge time series from 216 gages for a previously proposed SWOT orbit (970 km, 22 day repeat period and 78° inclination orbit with two 60 km swaths). For simplicity and solely for the purpose of estimating the impact of temporal sampling error, the Biancamaria et al. (2010) method assumed that SWOT measurements have already been converted to discharge. Furthermore, errors due to instantaneous estimation of discharge were not considered, though in reality they may be a significant component of the error budget. *In situ* discharge time series were used because they are much more readily available than water height. Since the errors in monthly discharge are expressed as percentages, the results should be somewhat similar to those for water height. Updated for the current orbit, the method of Biancamaria et al. (2010) gives a mean temporal sampling error for all 216 gages of 8.1%. On average, monthly mean temporal sampling errors decreased with increasing latitude, ranging from 10.0% around the equator to 6.1% above 60°N. For 11 large rivers distributed from the equator to the high latitudes, Papa et al. (2012)

showed that insufficiently frequent temporal sampling around the seasonal peak discharge can lead to substantial errors in mean river discharge computed over a satellite repeat period. For boreal rivers, nadir altimetry sampling with a repeat period longer than 20 days leads to errors >>20% due to the relatively large fraction of the annual discharge of boreal rivers that occurs over relatively short periods following ice breakup. Errors are much smaller using SWOT temporal sampling. Furthermore, considering the 11 rivers, SWOT temporal sampling errors are correlated to the discharge temporal variance contained in all frequencies above 1/(20 days) (R^2=0.87) rather than drainage area (R^2=0.18), at least for the few number of tested large rivers.

Unlike for rivers, there are not yet comprehensive studies estimating the impact of SWOT temporal sampling on measurement of variations in lake storage. However, given the fact that storage change in the large majority of global lakes remain entirely unobserved and that storage change in many observed lakes varies on seasonal or annual timescales (Crétaux et al., 2015), it is expected that the impacts of limited temporal sampling will be smaller than in the case of rivers.

In summary, despite the uneven time sampling and the limited regions that will not be sampled, SWOT will provide unprecedented observations of continental surface waters at global scale. The next sections review in more detail published studies that have explored, for different science questions, the benefits of the SWOT mission for land hydrology (section 2 for rivers, section 3.1 for lakes and reservoirs, and section 3.2 for other water bodies and specific applications).

2. River studies

2.1. Rivers seen by SWOT

SWOT will monitor the spatial and temporal dynamics of surface water globally, especially rivers. At a specific location, river stage, width, and velocity variations and therefore discharge depend on many local factors such as soil characteristics, bedrock characteristics, topographic variability, channel density, vegetation characteristics, and the space-time variability of precipitation, and drainage area, among other characteristics. SWOT will provide the first globally consistent and coherent images of river storage and discharge variations. Over the last two decades, optical imagery and digital elevation data have helped to map medium to large rivers, whereas airborne and local measurements have provided valuable information for smaller rivers (Lehner et al. 2008, Allen and Pavelsky 2015). SWOT will provide consistent and coherent information about the spatial distribution of river storage and discharge, which will especially improve the availability of information about rivers that are not well monitored because *in situ* observations are not collected or because they are not shared across political boundaries. In addition, SWOT will provide

405 critical information about the impact of river discharge characteristics and variations on human
406 societies. This includes the nature of floods and droughts in poorly monitored river basins and the
407 characteristics of discharge in rivers that cross international boundaries (transboundary basins).
408 Notwithstanding the profound improvement that SWOT will provide in the availability of
409 information about rivers globally, SWOT does not have the objective of and cannot be an *in situ*
410 gage network replacement. In most circumstances, *in situ* gages will be, by far, more precise than
411 any remote sensing discharge estimates. This is especially important for applications such as water
412 management, where highly accurate and precise information is required for legally significant
413 purposes. For example, data from the gauge on the Colorado River at Lees Ferry, AZ is used to
414 determine the allocation of water to surrounding states. SWOT will likely not be sufficiently
415 accurate for this purpose. On the other hand, stream gage information is by its nature local and does
416 not provide a full view of the spatial variations of streamflow. Moreover, some types of rivers such
417 as highly braided channels and rivers with poorly defined banks are not well-suited to *in situ* gauge
418 measurements. The main benefit of SWOT in this respect will be to provide new and
419 complementary 2D observations for a wide range of different river planforms. Clearly, SWOT will
420 not observe full river networks because it will be limited to measuring rivers 50-100 m in width.
421 Therefore, a key question is: what portions of the global river network SWOT will observe and
422 what improvement will it represent compared to current capabilities? Pavelsky et al. (2014a) have
423 addressed these questions. Using river networks from Hydro1k (Verdin and Greenlee 1998) and
424 HydroSHEDS (Lehner et al. 2008), the global *in-situ* gage discharge time series database from the
425 Global Runoff Data center (GRDC, http://www.bafg.de/GRDC/EN/Home/homepage_node.html)
426 and downstream hydraulic geometry (power law relationships between drainage area, mean annual
427 discharge and river width at sub-basin scales), they have quantified the fraction of global river
428 basins that SWOT would observe given river observability thresholds of 100 m and 50 m. They
429 found that SWOT would observe more than 60% of the global sub-basins with an area of 50,000
430 km^2 given the ability to observe rivers wider than 100 m. If SWOT can meet the goal of observing
431 50 m wide rivers, more than 60% of sub-basins with an area of 10,000 km^2 would be observed. For
432 the smallest river basins observed, only the mainstem river will likely be measured by SWOT.
433 For SWOT-observable rivers, a number of studies have investigated the potential to produce
434 river discharge estimates directly from SWOT water level, surface slope, and inundation extent
435 observations. We review these studies in section 2.2. In section 2.3, we review studies that have
436 pursued an alternate pathway of combining SWOT observations with hydrologic and river
437 hydrodynamic modeling to produce river discharge estimates.
438
439

2.2. Instantaneous direct river discharge estimations

Space-based observations of discharge began nearly two decades ago with the observation that variations in river width, observable from satellites, can be used along with limited *in situ* discharge data to develop rating curves (Smith et al. 1995, 1996, Smith 1997, Smith and Pavelsky 2008). A few years later, the first attempts were made to use nadir altimetry in conjunction with *in situ* observations to derive river discharge from altimetry-based water elevation data using rating curves (e.g. Kouraev et al. 2004). An alternative strategy of estimating discharge using water elevation, width, slope and velocity observed by or derived from spaceborne sensors was pursued in studies by Bjerklie et al. (2003) and Bjerklie et al. (2005) at about the same time. These attempts were specific to individual study reaches, were highly parametrized, and required ancillary *in situ* data in addition to altimetry-based variables. It was recognized that the next logical step was to develop discharge algorithms that could take advantage of all the information provided by SWOT (water elevations, slopes and inundation extent) so as to produce river discharge estimates at the scale of large river basins or even globally. Following the analysis by Pavelsky and Durand (2012) that new discharge algorithms specifically tuned for SWOT data need to be developed, four different discharge algorithms have been proposed to derive river discharge from SWOT. Characteristics of these algorithms are summarized in Table 3 and are briefly presented in the next paragraph. Gleason and Smith (2014) and Gleason et al. (2014) have pursued an approach that they termed At-Many-stations Hydraulic Geometry (AMHG hereafter). Bjerklie (2007) describes an approach (B2007 hereafter) that is based on an equation similar to the Manning equation with tuned power law coefficients. Garambois and Monnier (2015), hereafter GM2015, propose a method based on physical and numerical approximations of the Saint-Venant equations to invert the unobserved equivalent bathymetry and friction coefficient and then derive discharge. Durand et al. (2014) also use physical and numerical approximations (different than GM2015) of the Saint-Venant equations. This algorithm is referred to hereafter as ‘MetroMan’, because it uses the Manning equation along with the continuity equation and a Metropolis algorithm to invert bathymetry, friction and discharge. We discuss each of these algorithms, including hypotheses and limitations, briefly below. Additionally, these algorithms are summarized in Table 3.

The AMHG algorithm will use the intensive SWOT observations of river width to derive discharge using the well-known geomorphologic relationship between river width (w) and discharge (Q) at a specific location: $w=aQ^b$. The a and b coefficients are considered constant in time but vary along a given river. The innovation of the AMHG algorithm is based on the important fact (reported for the first time in Gleason and Smith 2014) that a and b at cross-sections within the same river reach commonly exhibit a well-defined log-linear relationship. Therefore, by considering width

variations at many cross-sections along a river in combination, the number of unknowns is decreased, allowing *a, b, and Q* to be estimated using a genetic algorithm requiring only multitemporal width observations at many river reaches (Gleason et al. 2014). A global parametrization is proposed by Gleason et al. (2014) when no a priori information is available. In this paper, the authors highlight a series of cases for which the algorithm will not work (corresponding to rivers that do not verify the conditions listed in column 'Tested river types' for this algorithm in Table 3). When these cases (types of rivers) are excluded, the relative Root Mean Square Error (RMSE) between AMHG and *in situ* discharge ranges from 26% to 41% for instantaneous discharge.

Bjerklie's algorithm (Bjerklie 2007) is based on a tuned Manning equation, using a constant river slope and parameterized Manning coefficient (*n*) varying in time and taking into account idealized channel shape. It requires as ancillary parameters the mean annual discharge (required because SWOT will provide surface water elevation and not river water depth). This method is robust if there are no floods and if the mean annual discharge is accurately known.

The GM2015 algorithm is a forward and inverse model based on the 1D Saint-Venant's equations applied to river reaches and rewritten to take into account SWOT measurements of water surface elevation, width and slope. It assumes no lateral inflows, steady-state flows at observation times, low Froude Number (<0.5, corresponding to neglecting the inertia term in the Momentum Equation), trapezoidal cross-section, and constant friction coefficient in time. The inverse model allows retrieval of discharge and an effective friction coefficient (Strickler or Manning coefficient) and cross sectional geometry for the lowest observed level (i.e. the low flow bathymetry), for a given set of observations. The identified coefficients (friction and cross section geometry) can then be used to compute discharge for other SWOT observations using the forward model. Garambois and Monnier (2015) tested the GM2015 algorithm on more than 90 synthetic rivers covering a wide range of conditions (width, depth, discharge) that will be observed by SWOT. They reported RMSE of discharge below 15% for first guess error exceeding 50% and a very robust estimation of discharge, as measurements errors and errors due to physical approximation are included in the estimated bathymetry and friction coefficient errors. Even if some equafinality (Beven 2006) exists between friction coefficients and bathymetry, the GM2015 algorithm seems to provide accurate estimates of equivalent bathymetry and friction in the range of tested discharge.

The MetroMan algorithm, like GM2015, uses an approximation (the diffusive wave approximation) of the 1D Saint-Venant equations. However, the mathematical implementation of the forward and inverse models are different, and it also takes into account unknown lateral inflows. It has been evaluated using a 22.4 km river reach of the Severn River (river width ~60 m) in the United Kingdom and one of its tributary for an in-bank flow event (duration 5 days) and an out-of-

bank flood event (duration 15 days). For the in-bank event, when lateral inflows from tributaries were known, discharge was retrieved with 10% RMSE, whereas when lateral inflows were unknown, the discharge RMSE went up to 36%. For the out-of-bank flood event with unknown lateral inflows, the RMSE was 19%. Both the GM2015 and MetroMan algorithms required multiple observations (at different times) of water surface height, width and slope (average over 1-10 km river reaches) and require substantial variability in water elevation and discharge across the observations. Bathymetry and friction affect river flows at different spatial scales. It worth noting that MetroMan and GM2015 retrieve these river parameters at the kilometer river reach scale and might therefore be slightly different from the ones estimated at the local scale.

Results from these investigations are encouraging and demonstrate the feasibility of retrieving river discharge from SWOT observations alone. Although these four algorithms were developed by different teams, their development was not independent as all author groups are members of the SWOT Science Definition Team (SDT) Discharge Algorithms Working Group. Intercomparison studies are currently being performed over different types of rivers and the relative strengths and weaknesses of each algorithm are being evaluated. Pending the results of these ongoing comparisons, the potential for implementation and performance of the algorithms at global scales is still an open question. Furthermore, at this point they have only been tested over non-braided rivers, whereas many large rivers (e.g. the Amazon, Ganges/Brahmaputra, and Ob') and many smaller rivers are at least partially braided. The precise river reaches to which the algorithms can be applied globally remain undefined but most likely will have lengths ranging from a few km to a few 10s of km. For those algorithms that require ancillary information and/or a first guess (see '1st guess/ancillary data' column in Table 3) this information will be defined and provided globally before launch. Finally, testing of algorithms with real SWOT data and realistic errors will be crucial for fully assessing the suitability of these algorithms.

2.3. Data assimilation and optimal interpolation

An alternate strategy for estimation of discharge and other water surface variables is the use of indirect and/or statistical methods. Work in this area falls into two categories: optimal interpolation (OI) to improve spatial/temporal coverage of SWOT water elevation and discharge estimates (Yoon et al. 2013 and Paiva et al. 2015) and data assimilation (DA), which uses SWOT data to correct hydraulic/hydrologic model parameters or state vectors (Andreadis et al. 2007, Durand et al. 2008, Biancamaria et al. 2011, Yoon et al. 2012, Andreadis and Schumann 2014, Pedinotti et al. 2014, Munier et al. 2015). Table 4 summarizes all these studies. All of the nine studies summarized were designed in the context of Observing System Simulation Experiments (OSSE), a methodology

545 designed to assess the potential of a new type of measurements before it is built or deployed. Figure
546 5 shows the conceptual framework of an OSSE in the context of SWOT studies using optimal
547 interpolation (a.) and data assimilation (b.). Among these nine studies, the OSSE consisted of first
548 computing time series of realistic states (water elevations and discharges) over a specified study
549 domain with a hydraulic or hydrologic model. This simulation is considered to be the "truth" in the
550 context of the OSSE (Figure 5). Then, a SWOT simulator is run to provide what the algorithm treats
551 as SWOT measurements. These so-called "virtual" or "synthetic" SWOT observations are then used
552 with OI or DA methods to improve the SWOT estimate of river discharge and/or related variables.
553 Comparison of these derived values to the "truth" allows quantification of the benefits of SWOT
554 data coupled with the dynamic model. In all studies included here, synthetic SWOT data have been
555 simulated with simple methods: SWOT spatio-temporal sampling is computed using SWOT orbit
556 and swath extents to sample "true" water elevations (or discharge for Paiva et al. 2015), to which
557 white noise (corresponding to instrument noise only) has been added. As the SWOT mission has
558 evolved through different design stages between 2007 and 2015, different orbits and swath extents
559 (e.g. no nadir gap) have been considered (see Table 4). Only Munier et al 2015 is recent enough to
560 consider the final SWOT nominal orbit presented in section 1.4. Furthermore, all of the studies have
561 been performed as twin experiments in which the same model has been used for computing the
562 "true" states and the "corrupted" ones (Figure 5).
563 Among the OI studies, Yoon et al. (2013) used local space-time ordinary kriging to estimate
564 water height between SWOT observation times over the Tennessee River. Their method used
565 hydrodynamic model outputs to compute the true heights. They obtained mean spatial and temporal
566 RMSE of 11 cm and 12 cm, respectively. However, when they used *in situ* gage time series as the
567 truth, the temporal RMSE increased to 32 cm. This difference is apparently due in part to effects of
568 water management, which are not taken into account in the hydrodynamic model. Paiva et al.
569 (2015) also used spatio-temporal OI but applied it to estimate discharge rather than water height.
570 They developed an innovative method termed River Kriging (RK), which analytically derives
571 space-time discharge covariance using the diffusive wave approximation to the Saint-Venant
572 equations. They showed, using the Ganges-Brahmaputra-Meghna Rivers system in Bangladesh, that
573 the RK method out-performed linear interpolation, simple kriging and ordinary kriging.
574 Furthermore, RK-interpolated daily discharge had accuracy similar to that of the initial SWOT
575 discharge time series. However, the method did not perform well when tidal forcing dominated the
576 discharge signal. Taken together, the Yoon et al. (2013) and Paiva et al. (2015) studies show the
577 potential to interpolate SWOT observations at daily time scales. However, they have been applied to
578 a very limited set of rivers to date.
579 DA techniques are increasingly being used in the framework of real time operations to forecast

water levels in the context of flooding (Bates et al. 2014), for real-time reservoir operations (Munier et al. 2015), for model calibration and parameter estimation (Bates et al. 2014) or for the purpose of reconstructing the history of some components of the continental water cycle (Reichle et al. 2014). All of these themes have been addressed by one or more of the SWOT DA studies referenced in Table 4. Andreadis et al. (2007) and Biancamaria et al. (2011) used virtual SWOT water depth measurements to correct water depth from river hydrodynamics models applied to the Ohio and Ob' Rivers, respectively. Assumptions included well-known bathymetry and no bias in water elevation measurements. They showed that in these two applications, model errors dominated and therefore assimilating SWOT (synthetic) data helped to decrease water depth error and consequently discharge estimates. These studies demonstrated the potential of SWOT data to improve forecasting of streamflow. Keeping in mind that the SWOT mission will likely not produce near real time products, these approaches nonetheless can be applied to producing discharge and water level products retrospectively once the SWOT data become available, especially with the use of a DA smoother (Biancamaria et al. 2011) that tends to smooth discontinuities before and after the assimilation time of an observation with a DA filter.

Flood forecasting is an area of hydrology particularly suited to the use of DA techniques. In these applications, model initial conditions are critical to producing accurate forecast. This was the motivation for the work of Andreadis and Schumann (2014) who developed methods of using satellite water elevation and water area (from nadir altimetry, Lidar, SAR imagery and SWOT) to correct initial conditions in an application of a hydrodynamic model to the Ohio River. They showed that using satellite observations improved water elevation and flood extent forecasts with lead times up to 10 days. For some flood events, however, model errors exceeded errors due to initial conditions after a few days, and the benefits of the assimilation dissipated. Additionaly, it has recently been shown that assimilating flood water level derived from SAR images combined with floodplain topography into a hydrodynamic modeling helps to improve flood forecasts (García-Pintado et al. 2013, García-Pintado et al. 2015).

Other studies have demonstrated the capability of using SWOT data to correct hydraulic model parameters (especially bathymetry, elevation, and slope; see Durand et al. 2008 and Yoon et al. 2012) or hydrologic model parameters (friction coefficients; see Pedinotti et al. 2014). Errors in the corrected parameters have decreased in some cases by more than 50% via DA. Of course, these results have to be interpreted carefully, as they are dependent on the model/observation errors used and the fact that they have been done in the context of model twin experiments, which often result in a benefit to DA-based methods in comparison with "real" applications. Nonetheless, these studies are promising and clearly show the potential benefits of SWOT data in conjunction with river hydrodynamic modeling even if the SWOT data are not delivered in near real time.

615 Finally, Munier et al. (2015), using DA in conjunction with an automatic control algorithm,
616 showed the potential of SWOT to improve management of the Selingue Reservoir in the upper
617 Niger River basin by optimizing reservoir releases to meet a minimum low flow requirement
618 upstream of the Niger Inner Delta. Their algorithm made use of SWOT data both for estimation of
619 reservoir storage and for discharge computation using a simplified river hydrodynamics model
620 applied to the reach downstream of the reservoir.
621 It should be highlighted that all the teams involved in the studies reported here are collaborating
622 at different levels. Members of the author groups that produced the papers reviewed in this section
623 met during the "Hydrologic Data Assimilation for the SWOT Mission" meeting, held on 12-13
624 November 2013 (Biancamaria et al. 2014) and further DA work in the next few years leading up to
625 launch of the SWOT mission is promising.
626
627 The studies reviewed in sections 2.1-2.3 show the benefits that can be expected from SWOT
628 measurements for better understanding river flow dynamics, from the river reach scale to the river
629 basin scale. New and innovative techniques have already been developed that can exploit SWOT
630 data, and these methods will be available from the beginning of the mission to ensure quick use and
631 science return of SWOT data. However, more work is still needed, especially to explore the
632 implications of SWOT errors, which have been represented to date using highly simplifying
633 assumptions. SWOT errors will be much more complex than white noise. In particular, the impacts
634 of layover, water classification errors, wet troposphere effects, and correlated instrument error along
635 the swath are topics of immediate relevance that currently are being investigated.
636
637 3. Lake/reservoir studies and other land hydrology applications
638
639 Section 2 summarized SWOT river-related studies with a focus on river discharge estimation
640 (both directly and through data assimilation). Lakes and reservoirs have been somewhat less studied
641 as shown in Table 5, which summarizes SWOT-related lake and reservoir studies. Compared to the
642 five SWOT discharge algorithms papers and nine DA/OI papers, there are only three papers that
643 consider lakes and/or reservoirs in the context of SWOT. This is in part due to the fact that the main
644 SWOT lake/reservoir product, storage change estimation of all observed lakes and reservoirs, is
645 more easily derived from SWOT direct measurements (maps of water elevations and water surface
646 extent), than is river discharge. Nonetheless, SWOT has important implications for understanding
647 the dynamics of individual lakes and reservoirs and their part in the land surface water budget. The
648 mission is expected to lead to a major leap in our understanding of these water bodies. For instance,
649 storage variations in reservoirs globally, which have been estimated to have produced a "drag" on

sea level rise of about 0.5 mm/yr or around 1/6 of observed sea level rise, are so poorly estimated that the sign of this term is no longer known due to slowing of global reservoir construction and filling of existing reservoirs with sediment (Lettenmaier and Milly, 2009).

Furthermore, SWOT will not only observe rivers and lakes/reservoirs, but also all other water bodies on the continents and at their interfaces with the oceans: wetlands, stream-aquifer interfaces, estuaries and ice sheets. In particular, it will be a tremendous source of information for transboundary river basins, which are a challenge for water managing between upstream and downstream countries. More generally, SWOT will observe the direct human impact on the continental water cycle and therefore will have scientific but also societal and political implications.

3.1. Lakes and reservoirs

There is currently large uncertainty concerning the global distribution of lakes (Downing et al. 2006, Verpoorter et al. 2014) and the variations of water stored in them. The locations of largest lakes are, of course, well known and monitored. It is also well known that the majority of lakes are located at high latitudes (above 50°N; Lehner and Döll 2004). However there is still considerable uncertainty concerning the number of medium and small lakes, even aside from their spatial and temporal dynamics. For example, according to Downing et al. (2006), based on multiple databases and extrapolation for smaller lakes, there are slightly more than 300 million lakes globally with surface area exceeding 0.001 km^2, most of which (99.87% in number and 43% in area) have surface areas less than 1 km^2. However, the numbers of small lakes in Downing et al. (2006) are inferred from the distribution of larger lakes rather than being directly observed, so this estimate is highly uncertain. In contrast, Verpoorter et al. (2014) report, using Landsat imagery, about 117 million lakes with surface areas that exceed 0.002 km^2, a predominance of which have areas between 0.1 and 1 km^2). However, the use of Landsat imagery (which has a pixel size of 30 m) tends to underestimate small water bodies, especially those that cover less than about 10 Landsat pixels, or about 0.01 km^2. Furthermore, it is difficult to classify water surfaces at the global scale automatically because of clouds, cloud shadow, the use of images acquired at different dates, differences in lake turbidity, and other factors, all of which add uncertainty to current estimates of the global distribution of lakes by area. In addition, it is very difficult to automatically differentiate the smallest lakes observable in Landsat imagery from segments of partially detected rivers. Finally, all of the current global lakes databases (e.g. Lehner and Döll 2004, Verpoorter et al. 2014) are static and do not provide any information about spatio-temporal dynamics, notwithstanding well-known studies of long-term variations in the surface areas of both large (e.g. Gao et al. 2012) and small (e.g. Smith et al. 2005) lakes. SWOT will provide revolutionary information concerning lake

685 extent and water storage, which will be beneficial not just for a better understanding of the
686 continental hydrological cycle but also for the carbon (Cole et al. 1994) and methane (Walter et al.
687 2007) cycles at continental and global scales.
688 If the global distribution of lakes is subject to large uncertainties, their water elevation changes
689 are even less well known. Therefore, estimating total water storage change of all lakes remains a
690 challenge. Biancamaria et al. (2010) have provided early estimates. Using, annual water level
691 amplitudes from 224 lakes worldwide, they found no clear correlation between annual water level
692 variations and lake area or lake drainage area. Rather, it seemed that inter-annual water surface
693 amplitudes followed a log-normal distribution, which they used to estimate water level variations
694 for all lakes globally. They used a power-law relationship between the number of lakes and lake
695 area derived by Downing et al. (2006) to compute the number of all lakes and their size. By
696 performing a very rough approximation of cylindrical lake bathymetry, using the previously
697 mentioned lake log-normal water level distribution, the Downing et al. (2006) lake numbers versus
698 lake areas relationship, they were able to compute cumulative lake storage change as a function of
699 lake area and, ultimately, the total annual lake storage change (about 9,000 km^3). Their computation
700 was based on just one realization of the log-normal water level distribution for each lake area bin
701 and did not consider uncertainty due to the random distribution. In order to take this uncertainty into
702 account, 100 realizations of the log-normal water level distribution have been generated for each
703 lake area bin. For each realization the same methodology of Biancamaria et al. (2010), previously
704 described, has been applied. Figure 6 shows the updated results with the ensemble of 100
705 realizations (grey curves). The mean of this ensemble, which is likely a better approximation of the
706 cumulative annual lake storage change than a single realization of the log-normal distribution, is
707 represented by the green curve on Figure 6. The ensemble mean is close to the cumulative storage
708 change published by Biancamaria et al. (2010), while the ensemble spread clearly shows the
709 uncertainty associated with the log-normal water level distribution approximation. Of course, there
710 are also errors from the number of lakes versus lake area power law and the cylindrical bathymetry
711 approximation, which add (unrepresented) errors to the annual storage change estimates at global
712 scale. It should be noted that these errors are extremely difficult to estimate and have yet to be
713 modeled.
714 Currently, storage change can be computed for the small number of lakes for which *in situ* data
715 are freely available. The alternative is to use satellite data to derive water elevation (from nadir
716 altimeters or Lidar) and surface extent (from optical or SAR sensors) (Gao et al. 2012, Zhang et al.
717 2014, Arsen et al. 2014, Baup et al. 2014, Crétaux et al. 2015). However, these approaches require
718 data from at least two different satellites, nearly always at different observation times, with different
719 space-time resolutions. As such, they require significant manual editing of the time series

720 (especially for water elevation) and are challenging to apply automatically at large scales. The
721 resolution of current nadir altimeters also limits the application of these methods. Satellite
722 capability to monitor specific lakes depends on not just the radar footprint on the ground but also
723 the lake shape. Current results (for example, from the Hydroweb database, http://www.legos.obs-
724 mip.fr/en/soa/hydrologie/hydroweb/) show that 10 km^2 lake area (dashed red line on Figure 6) is, on
725 average, a good guess for the minimum lake extent that nadir altimeters can observe, though some
726 results can be obtained for smaller lakes (Baup et al. 2014). Considering the constellation of
727 satellites that are the most likely to fly in the near future (AltiKa, Jason-3, Sentinel-3A and -3B),
728 based on the distribution shown in Figure 6 (green curve) and assuming that these satellites will
729 sample all lakes above 10 km^2 area that are intersected by their nadir ground tracks (which is a very
730 optimistic hypothesis), then only 36% of the total annual storage change can be measured (as not all
731 lakes above 10 km^2 will be observed). In contrast, SWOT, should be able to monitor about 65% of
732 total annual storage change (Biancamaria et al. 2010). On Figure 6, all lakes above 250m x 250m or
733 about 0.06 km^2 (blue dashed line) account for 68% of the total annual storage change, but SWOT
734 will miss a small fraction of these lakes. This is due to measurement errors that could be higher than
735 the annual water level amplitude for some lakes in between 0.06 km^2 and 1 km^2. However, SWOT
736 should overcome most of the uncertainty in the lake spatial distribution (grey curves on Figure 6), at
737 least for lakes with an area above 0.06 km^2. To assess the accuracy that could be expected from
738 SWOT-derived lake storage changes, Lee et al. (2010) performed an OSSE for Arctic lakes, using a
739 methodology similar to the one presented in section 2.3 for optimal interpolation and shown on
740 Figure 5a. Based on daily interpolated lake level variations from altimetry, satellite optical images
741 and parametrizations, daily water level variations for several thousands of lakes in the Peace-
742 Athabasca Delta (Canada), Northern Alaska (US) and West Siberia (Russia) were derived and used
743 as the "truth". With this data set, they estimated that at high latitudes, SWOT lake storage change
744 measurements will likely have errors lower than 5% for lakes larger than 1 km^2, whereas errors for
745 lakes with areas of 0.01 km^2 should be around 20%, confirming the relatively high accuracy that is
746 expected from SWOT data. However, this study did not consider measurements errors due to
747 layover, water classification, wet troposphere… (see section 1.3). Work on a more limited number
748 of lakes in the Peace-Athabasca Delta suggests that errors in water surface elevation will dominate
749 the calculation of storage change measurements in comparatively large lakes, while errors in
750 inundated area will play a more important role for storage change calculations in small lakes (Smith
751 and Pavelsky, 2009).
752 Reservoirs also play an important role in the continental water cycle. Zhou et al. (in review)
753 showed, using a large scale water management model, that 166 of the world's largest reservoirs,
754 which have a total storage capacity of 3900 km^3 (~60% of all reservoirs storage), could have almost

700 km^3 seasonal storage variation (~10% of the total reservoirs storage). Despite this significant variability, there is only the study of Munier et al. (2015) that has investigating the potential of SWOT for reservoirs monitoring (see section 2.3). This study showed the potential use of SWOT reservoir measurements to optimize reservoir operations. Gao et al. (2012) and Crétaux et al. (2015) have shown the feasibility of computing storage change for large reservoirs using nadir altimetry, which is very promising for SWOT. The lack of knowledge of the distribution of small lakes is also true for reservoirs. Even with global datasets for reservoirs, like the one compiled by the International Commission on Large Dams (ICOLD) or the Global Reservoir and Dam (GRanD) database (Lehner et al. 2011), there is little information for intermediate and small reservoirs. Given gaps in current understanding of the number and area distribution of lakes and reservoirs, SWOT will provide a major improvement in the ability to observe the dynamics of these water bodies directly. In particular, it will help to better characterize the role of small lakes and reservoirs at global scales, which are mostly ignored in current estimates of the dynamics of land water storage (Zhou et al. in review).

3.2. Other Land hydrology applications and synergistic land sciences

To date, published studies concerning SWOT have been mostly focused on understanding and assessing benefits of the new type of measurements that will be produced for river and lakes dynamics. This focus was essential as the mission was in an early stage of definition. Nonetheless, a number of other applications of SWOT data are expected in the land hydrology arena (Durand et al. 2010, Fu et al. 2012, Rodríguez 2015). One of these is the management of water in transboundary river basins. These basins cross one or more international boundaries and imply sharing of water, which in many cases can lead to tensions between upstream and downstream countries. Transboundary river basins are important globally, as they cover around 45% of the global land area, involve 145 countries and 40% of the total human population (Wolf et al. 1999). Clark et al. (2015, accepted) have reviewed studies using nadir altimetry for three transboundary basins (the Brahmaputra-Ganges-Meghna, the Indus and the Niger basins) and highlighted the importance of upcoming SWOT data for providing freely available observations of storage change, water level and discharge over the entire basin areas (not including the minor observations gaps discussed in section 1.4) repetitively and independently from national networks.

Another field that will greatly benefit from SWOT data will be the study of the direct impact of human activities (like water management infrastructures and water withdrawals) on the land hydrological cycle. For example, reservoirs (Shiklomanov and Lammers 2009) and soil changes and erosion (Descroix et al. 2012) can have important impacts on downstream river discharge, and these

impacts will be observed and may be quantifiable by SWOT. SWOT will also provide valuable information to model development and validation, especially for land surface models used in numerical weather prediction and climate models. Most such models at present only represent natural rivers. SWOT observations may also have application to studies of stream-aquifer exchanges at basin and continental scales, filling a current observation gap (Flipo et al. 2014).

SWOT will also provide useful data in wetland environments, although the range of observable wetlands remains uncertain. In wetlands with sparse vegetation and large extents of open water it is likely that SWOT will provide useful measures of water surface elevation and inundation extent. Where vegetation is denser, it remains unclear to what extent SWOT will be affected by scattering and layover caused by the vegetation. However, given difficulties in measuring the hydrology of large wetlands *in situ* and their importance in the global carbon and methane cycles, SWOT measurements may provide substantial benefits even if sampling under dense vegetation proves limited. Experiments to better define the opportunities and constraints of SWOT wetland measurements are, as of this writing, in the final planning stages. They will use measurements from AirSWOT (Rodriguez et al. 2010), to better understand SWOT returns from inundated vegetation.

Complementary to land hydrology, some additional science objectives for SWOT, referred to as synergistic sciences (Fu et al. 2012, Rodríguez 2015), have been identified, including:

- Freshwater/marine interfaces, especially in estuaries. This issue bridges ocean and continental hydrology and, while it is a key component of the hydrological cycle, it is just beginning to be addressed in the context of SWOT.
- Antarctic and Greenland ice sheet topographic variability. As shown on Figure 3, most of Greenland (which extends up to 82°N) and a substantial portion of Antarctica (and all its coastal regions) will be sampled at the highest time sampling frequency. However, it should be noted that SWOT performance over ice and snow is not yet well characterized (Fjørtoft et al. 2014). In addition, it is likely that SWOT data for many portions of these ice sheets will be available only at the lower resolution used for SWOT ocean products.
- Helping to characterize snow cover variability and, perhaps, help to characterize land cover variability.
- Estimation of vertical deflection due to gravity changes over large lakes.

These are just some of the anticipated SWOT scientific applications that have yet to be investigated in any substantial detail. Because most of these applications are synergistic to SWOT's principal scientific goals and because SWOT observing technology is not optimized for them, more investigations are needed to determine how useful SWOT data will be. For example, better characterization of Ka-band backscatter over snow and ice is needed (this also has implications for observations of high latitude rivers during ice breakup). In addition, for most new satellite

825 technologies like SWOT, applications not yet anticipated will emerge once the data becomes
826 available.
827
828
829 4. Conclusions and perspectives
830
831 We have described the characteristics of the upcoming wide swath altimetry satellite mission,
832 SWOT, and have reviewed recent published papers that have evaluated key scientific hydrology
833 uses of SWOT data. We argue that SWOT will be transformational for land hydrology in providing
834 fundamental information about rivers, lakes, and wetlands that has never before been available
835 directly from observations. The SWOT mission will provide, for instance, maps of surface water
836 elevation and their temporal evolution, therefore providing for the first time estimates of surface
837 water storage and fluxes at global scale for rivers wider than 50-100.
838 It will also characterize spatio-temporal variability of lakes and reservoirs with areas larger than
839 ~0.06 km^2, implying direct estimates of about 2/3 of global lake and reservoir storage variations
840 (current nadir altimeters provide estimates in both cases that represent less than 20 percent of the
841 total). Some of the types of studies for which SWOT data will be especially well suited are:
842 - global water balance studies,
843 - flood dynamics for medium to large rivers, especially those that persist for multiple SWOT
844 revisits,
845 - studies of surface water in the global carbon and methane cycles,
846 - documentation and quantification, of direct human impacts on the hydrological cycle.
847 With respect to Earth system modeling, it will provide constraints and diagnostics that will allow
848 better representation of processes such as flood dynamics and human influence on the water cycle,
849 which at present are poorly quantified in global coupled land-atmosphere-ocean models. For
850 example, most such models do not represent the storage of water in man-made reservoirs, or its
851 effect on river discharge (Wood et al. 2011). SWOT will also have important societal impacts on
852 understanding of transboundary river basins; in many such cases, data about river discharge and
853 reservoir storage are not shared among upstream and downstream countries, and in this respect the
854 SWOT data, which will be freely available, will be transformational.
855 However, there is still much to be learned before the planned launch of the mission some five
856 years from the time of this writing. One priority must be to strengthen the results of studies
857 performed to date, especially by taking into account more realistic quantifications of the magnitudes
858 and types of SWOT measurement errors (e.g., spatially-correlated instrumental noise, error due to
859 the roll of the satellite, wet troposphere errors, water classification errors, topography and

vegetation errors, among others). These errors will be chiefly explored using two complementary tools: an increasingly sophisticated high-resolution SWOT simulator and AirSWOT airborne campaigns, which will provide SWOT-like measurements that can be compared to simultaneous ground validation data. To compute river discharge, four algorithms have been proposed, and they need to be investigated on diverse real cases, especially braided rivers. They also require a priori information such as river bathymetry and friction coefficients. The sensitivity of discharge estimates to the accuracy of these a priori parameters should be estimated, and they should be computed at a global scale prior to launch.

Furthermore, synergies with other satellite missions observing different component of the water cycle that are likely to collect data simultaneously with SWOT should be investigated, to improve understanding of the water cycle as a whole. Results from discussion of the SWOT Science Definition Team to date suggest that data assimilation approaches are not yet mature enough for global application. For this reason, studies like those reviewed in section 2.2 are based on the need for simple algorithms, which can be applied more or less directly to SWOT observations of river water levels, slopes, and widths to estimate discharge. However, some recent studies (Yamazaki et al. 2011, Neal et al. 2012, Schumann et al. 2013, Bates et al. 2014) suggest that application of river hydrodynamics models have advanced to the point that applications of these models (which would be the physics core for data assimilation algorithms) may now be feasible at continental and global scales (Wood et al. 2011, Schumann et al. 2014, Bierkens et al. 2015). Thus, the role of data assimilation in SWOT river discharge and related variables may need to be revisited.

Finally, some thinking about the successor of SWOT is now appropriate. If SWOT is successful, it almost certainly will motivate demand for continuing observations, in the same way that the first ocean altimeter, TOPEX/Poseidon, did for ocean sciences. With the launch date of SWOT approaching quickly, it is not too early to think about how a future mission might extend and improve on results from SWOT.

Acknowledgments

SB acknowledges funding from the CNES Terre-Océan-Surfaces Continentales-Atmosphère (TOSCA) commity for the SWOT Science Definition Team. DL acknowledges funding from NASA Earth Sciences, Grant No. NNX15AF01G. TP's work on this paper was supported by NASA Terrestrial Hydrology Program Grant No. NNX13AD05G and by funding from the SWOT Project at the NASA/Caltech Jet Propulsion Lab.

We thank two anonymous reviewers and Pierre-Andre Garambois for their comments, which we believe have improved the manuscript.

This paper originated with presentations at the International Space Science Institute (ISSI) *Workshop on Remote Sensing and Water Resources*, held in Bern (Switzerland), 6-10 October 2014.

References

Allen GF, Pavelsky TM (2015) Patterns of river width and surface area revealed by satellite-derived North American River Width data set. Geophys Res Lett 42(2):295-402. doi:10.1002/2014GL062764

Alsdorf DE, Lettenmaier DP, Vörösmarty C (2003) The need for global, satellite-based obervations of terrestrial surface waters. EOS Trans Am Geophys Union 84(29):269-276. doi:10.1029/2003EO290001

Alsdorf DE, Lettenmaier DP (2003) Tracking fresh water from space. Science 301:1485-1488

Alsdorf DE, Rodríguez E, Lettenmaier DP (2007) Measuring surface water from space. Rev Geophys 45(2):RG2002. doi:10.1029/2006RG000197

Andreadis KM, Clark EA, Lettenmaier DP, Alsdorf DE (2007) Prospects for river discharge and depth estimation through assimilation of swath-altimetry into a raster-based hydrodynamics model. Geophys Res Lett 34:L10403

Andreadis KM, Schumann GJP (2014) Estimating the impact of satellite observations on the predictability of large-scale hydraulic models. Adv Water Resour 73:44-54. doi:10.1016/j.advwatres.2014.06.006

Arsen A, Crétaux JF, Berge-Nguyen M (2014) Remote sensing-derived bathymetry of lake Poopo. Remote Sens 6(1):407-420. doi:10.3390/rs6010407

Bates PD, Neal JC, Alsdorf DE, Schumann GJP (2014) Observing global surface water flood dynamics. Surv Geophys 35(3):839-852. doi:10.1007/s10712-013-9269-4

Baup F, Frappart F, Maubant J (2014) Combining high-resolution satellite images and altimetry to estimate the volume of small lakes. Hydrol Earth Syst Sci 18:2007-2020. doi:10.5194/hess-18-2007-2014

Beven K (2006) A manifesto for the equifinality thesis. J Hydrol 320(1-2):18-36. doi:10.1016/j.jhydrol.2005.07.007

Biancamaria S, Andreadis, KM, Durand MT, Clark EA, Rodriguez E, Mognard NM, Alsdorf DE, Lettenmaier DP, Oudin Y (2010) Preliminary characterization of SWOT hydrology error budget and global capabilities. IEEE J Sel Top Appl Earth Obs Remote Sens 3(1):6–19. doi:10.1109/JSTARS.2009.2034614

Biancamaria S, Durand MT, Andreadis K, Bates PD, Boone A, Mognard NM, Rodriguez E, Alsdorf DE, Lettenmaier DP, Clark EA (2011) Assimilation of virtual wide swath altimetry to improve Arctic river modelling. Remote Sens Environ 115(2):373–381. doi:10.1016/j.rse.2010.09.008

Biancamaria S, Andreadis K, Ricci S (2014) Using images of continental water surface Elevations from upcoming satellite mission. EOS Trans Am Geophys Union 95(12) :105.

946 doi:10.1002/2014EO120004
947
948 Bierkens MFP, Bell VA, Burek P, Chaney N, Condon LE, David CH, de Roo A, Döll P, Drost N,
949 Famiglietti JS, Flörke M, Gochis DJ, Houser P, Hut R, Keune J, Kollet S, Maxwell RM, Reager JT,
950 Samaniego L, Sudicky E, Sutanudjaja EH, van de Giesen N, Winsemius H, Wood EF (2015) Hyper-
951 resolution global hydrological modelling: what is next? Everywhere and locally relevant. Hydrol
952 Process 29(2):310-320. doi:10.1002/hyp.10391
953
954 Bjerklie DM, Dingman SL, Vörosmarty CJ, Bolster CH, Congalton R (2003) Evaluating the
955 potential for measuring river discharge from space. J Hydrol 278(1):17-38. doi:10.1016/S0022-
956 1694(03)00129-X
957
958 Bjerklie DM, Moller D, Smith LC, Dingman SL (2005) Estimating discharge in rivers using
959 remotely sensed hydraulic information. J Hydrol 309(1-4):191-209.
960 doi:10.1016/j.jhydrol.2004.11.022
961
962 Bjerklie DM (2007) Estimating the bankfull velocity and discharge for rivers using remotely sensed
963 river morphology information. J Hydrol 341(3-4):144-155. doi:10.1016/j.jhydrol.2007.04.011
964
965 Blöschl G, Sivapalan M (1995) Scale issues in hydrological modelling: A review. Hydrol Process
966 9(3-4):251-290. doi:10.1002/hyp.3360090305
967
968 Clark EA, Biancamaria S, Hossain F, Crétaux JF, Lettenmaier DP (accepted) Current and future
969 application for altimetry in trans-boundary river management. In: Benveniste J, Vignudelli S,
970 Kostianov AG (ed) Inland Water Altimetry, Springer, ISBN 978-3-642-22678-6 (should be
971 published in 2015)
972
973 Crétaux JF, Biancamaria S, Arsen A, Bergé-Nguyen M, Becker M (2015) Global surveys of
974 reservoirs and lakes from satellites and regional application to the Syrdarya river basin. Environ Res
975 Lett 10(1):015002. doi :10.1088/1748-9326/10/1/015002
976
977 Crétaux JF, Jelinski W, Calmant S, Kouraev A, Vuglinski V, Berge-Nguyen M, Gennero M-C,
978 Abarca Del Rio R, Cazenave A, Maisongrande P (2011) SOLS: A lake database to monitor in the
979 Near Real Time water level and storage variations from remote sensing data. Advances in Space
980 Research 47(9): 1497-1507. doi:10.1016/j.asr.2011.01.004
981
982 Cole JJ, Caraco NF, Kling GW, Kratz TK (1994) Carbon-dioxide supersaturation in the surface
983 waters of lakes. Science 265(5178):1568-1570. doi:10.1126/science.265.5178.1568
984
985 Descroix L, Genthon P, Amogu O, Rajot JL, Sighomnou D, Vauclin M (2012) Change in Sahelian
986 Rivers hydrograph: the case of the recent red floods of the Niger River in the Niamey region. Glob
987 Planet Change 98-99:18-30. doi:10.1016/j.gloplacha.2012.07.009
988
989 Desjonquères JD, Carayon G, Steunou N, Lambin J (2010) Poseidon-3 Radar Altimeter: new modes
990 and in-flight performances. Marine Geodesy 33(S1):53-79. doi:10.1080/01490419.2010.488970
991
992 Downing JA, Prairie YT, Cole JJ, Duarte CM, Tranvik LJ, Striegl RG, McDowell WH, Kortelainen
993 P, Caraco NF, Melack JM, Middelburg JJ (2006) The global abundance and size distribution of
994 lakes, ponds, and impoundments. Limnol Oceanogr, 51(5):2388-2397.
995 doi:10.4319/lo.2006.51.5.2388
996
997 Durand MT, Andreadis KM, Alsdorf DE, Lettenmaier DP, Moller D, Wilson M (2008) Estimation

of bathymetric depth and slope from data assimilation of swath altimetry into a hydrodynamic model. Geophys Res Lett 35:L20401. doi:10.1029/2008GL034150

Durand MT, Fu LL, Lettenmaier DP, Alsdorf DE, Rodríguez E, Esteban-Fernandez D (2010) The Surface Water and Ocean Topography mission: Observing terrestrial surface water and oceanic submesoscale eddies. Proc IEEE 98(5): 766-779. doi:10.1109/JPROC.2010.2043031

Durand MT, Neal J, Rodríguez E, Andreadis K, Smith L, Yoon Y (2014) Estimating reach-averaged discharge for the River Severn from measurements of river water surface elevation and slope. J Hydrol 511:92-104. doi:10.1016/j.jhydrol.2013.12.050

Enjolras VM, Rodríguez E (2009) An assessment of a Ka-band radar interferometer mission accuracyover Eurasian Rivers. IEEE Trans Geosci Remote Sens 47(6):1752-1765. doi:10.1109/TGRS.2008.2006370

Farr TG, Rosen PA, Caro E, Crippen R, Duren R, Hensley S, Kobrick M, Paller M, Rodríguez E, Roth L, Seal D, Shaffer S, Shimada J, Umland J, Werner M, Oskin M, Burbank D, Alsdorf D (2007) The shuttle radar topography mission. Rev Geophys 45(2):R2004. doi:10.1029/2005RG000183

Flipo N, Mouhri A, Labarthe B, Biancamaria S, Rivière A, Weill P (2014) Continental hydrosystem modelling: the concept of nested stream-aquifer interfaces. Hydrol Earth Syst Sci 18(8):3121-3149. doi :10.5194/hess18-3121-2014

Fjørtoft R, Gaudin JM, Pourthié N, Lalaurie JC, Mallet A, Nouvel JF, Martinot-Lagarde J, Oriot H, Borderies P, Ruiz C, Daniel D (2014) KaRIn on SWOT: characteristics of near-nadir Ka-band interferometric SAR imagery. IEEE Trans Geosci Remote Sens 52(4):2172-2185. doi: 10.1109/TGRS.2013.2258402

Fu LL, Rodríguez E (2004) High-resolution measurement of ocean surface topography by radar interferometry for oceanographic and geophysical applications. In: Sparks RSJ, Hawkesworth CJ (ed) The State of the Planet: Frontiers and Challenges in Geophysics. Geophysical Monograph 150, AGU, Washington DC, pp. 209-224

Fu LL, Alsdorf DE, Morrow R, Rodríguez E, Mognard NM (2012) SWOT: the Surface Water and Ocean Topography Mission. JPL Publication 12-05. http://swot.jpl.nasa.gov/files/swot/SWOT_MSD_1202012.pdf. Accessed 20 February 2015

Gao H, Bohn TJ, Podest E, McDonald KC, Lettenmaier DP (2011) On the causes of the shrinking of Lake Chad. Environ Res Lett 6(3):034021. doi:10.1088/1748-9326/6/3/034021

Gao H, Birkett C, Lettenmaier DP (2012) Global monitoring of large reservoir storage from satellite remote sensing. Water Resour Res 48(9):W09504. doi:10.1029/2012WR012063

Garambois PA, Monnier J (2015) Inference of effective river properties from remotely sensed observations of water surface. Adv Water Resour 79:103-120. doi:10.1016/j.advwatres.2015.02.007

García-Pintado J, Neal JC, Mason DC, Dance S, Bates PD (2013) Scheduling satellite-based SAR acquisition for sequential assimilation of water level observations into flood modelling. J Hydrol, 495, 252-266. doi:10.1016/j.jhydrol.2013.03.050

García-Pintado J, Mason DC, Dance SL, Cloke HL, Neal JC, Freer J, Bates PD (2015) Satellite-

supported flood forecasting in river networks: A real case study. J Hydrol, 523, 706-724. doi:10.1016/j.jhydrol.2015.01.084

Gleason CJ, Smith LC (2014) Toward global mapping of river discharge using satellite images and at-many-stations hydraulic geometry. PNAS 111(13):4788-4791

Gleason CJ, Smith LC, Lee J (2014) Retrieval of river discharge solely from satellite imagery and at-many-stations hydraulic geometry: sensitivity to river form and optimization parameters. Water Resour Res 50(12):9604-9619. doi:10.1002/2014WR016109

Kouraev AV, Zakharova EA, Samain O, Mognard NM, Cazenave A (2004) Ob' river discharge from TOPEX/Poseidon satellite altimetry (1992–2002). Remote Sens Environ 93(1–2):238–245. doi:10.1016/j.rse.2004.07.007

Lee H, Durand MT, Jung HC, Alsdorf D, Shum CK, Sheng Y (2010) Characterization of surface water storage changes in Arctic lakes using simulated SWOT measurements. Int J Remote Sens 31(14):3931-3953. doi:10.1080/01431161.2010.483494

Lehner B, Döll, P (2004) Development and validation of a global database of lakes, reservoirs and wetlands. J Hydrol 296:1-22. doi:10.1016/j.jhydrol.2004.03.028

Lehner B, Verdin K, Jarvis A (2008) New global hydrography derived from spaceborne elevation data. EOS Trans Am Geophys Union 89(10):93-94. doi:10.1029/2008EO100001

Lehner B, Reidy Liermann C, Revenga C, Vörösmarty C, Fekete B, Crouzet P, Döll P, Endejan M, Frenken K, Magome J, Nilsson C, Robertson JC, Rödel R, Sindorf N, Wisser D (2011) High-resolution mapping of the world's reservoirs and dams for sustainable river-flow management. Front Ecol Environ 9(9):494-502. doi:10.1890/100125

Lettenmaier DP, Milly PCD (2009) Land waters and sea level. Nat Geosci 2(7):452-454. doi:10.1038/ngeo567

Mersel MK, Smith LC, Andreadis KM, Durand MT (2013) Estimation of river depth from remotely sensed hydraulic relationships. Water Resour Res 49(6):3165-3179. doi:10.1002/wrcr.20176

Moller D, Esteban-Fernandez D (2015) Near-nadir Ka-band field observations of fresh water bodies. In: Lakshmi V, Alsdorf D, Anderson M, Biancamaria S, Cosh M, Entin J, Huffman G, Kustas W, van Oevelen P, Painter T, Parajka J, Rodell M, Rüdiger C (ed) Remote Sensing of the Water Cycle. AGU Geophysical Monograph, 206, Wiley, New York, pp 143-155

Munier S, Polebistki A, Brown C, Belaud G, Lettenmaier DP (2015) SWOT data assimilation for operational reservoir management on the upper Niger River Basin. Water Resour Res 51. doi:10.1002/2014WR016157

National Research Council (2007) Earth Science and Applications From Space: National Imperatives for the Next Decade and Beyond. National Academies Press, Washington DC

Neal JC, Schumann GJP, Bates PD (2012) A subgrid channel model for simulating river hydraulics and floddplain inundation over large and data sparse areas. Water Resour Res 48:W11506. doi:10.1029/2012WR012514

Paiva RCD, Durand MT, Hossain F (2015) Spatiotemporal interpolation of discharge across a river

network by using synthetic SWOT satellite data. Water Resour Res 51. doi:10.1002/2014WR015618

Papa F, Biancamaria S, Lion C, Rossow WB (2012) Uncertainties in mean river discharge estimates associated with satellite altimeters temporal sampling intervals: a case study for the annual peak flow in the context of the future SWOT hydrology mission. IEEE Geosc Rem Sens Lett 9(4):569-573. doi:10.1109/LGRS.2011.2174958

Pavelsky T M, Durand MT (2012) Developing new algorithms for estimating river discharge from space. EOS Trans Am Geophys Union 93(45):457. doi:10.1029/2012EO450006

Pavelsky, TM, Durand MT, Andreadis KM, Beighley RE, Paiva RCD, Allen GH, Miller ZF (2014a) Assessing the potential global extent of SWOT river discharge observations. J Hydrol 519:1516-1525. doi:10.1016/j.jhydrol.2014.08.044

Pavelsky TM (2014b) Using width-based rating curves from spatially discontinuous satellite imagery to monitor river discharge. Hydrol Process 28(6):3035-3040. doi:10.1002/hyp.10157

Pedinotti V, Boone A, Ricci S, Biancamaria S, Mognard NM (2014) Assimilation of satellite data to optimize large-scale hydrological model parameters : a case study for the SWOT mission. Hydrol Earth Syst Sci 18(11):4485-4507. doi:10.5194/hess-18-4485-2014

Reichle RH, De Lannoy GJM, Forman BA, Drapper CS, Liu Q (2014) Connecting satellite observations with water cycle variables through land data assimilation: examples using the NASA GEOS-5 LDAS. Surv Geophys 35:577-606. doi:10.1007/s10712-013-9220-8.

Rodríguez E (2015) Surface Water and Ocean Topography Mission (SWOT), Science Requirements Document. JPL document D-61923. https://swot.jpl.nasa.gov/files/swot/SRD_021215.pdf. Accessed 20 February 2015

Rodriguez E, Moller D, Smith LC, Pavelsky TM, Alsdorf DE (2010) AirSWOT: an airborne monitoring platform for surface water monitoring. AGU Fall Meeting Abstract #H32D-06.

Schumann GJP, Neal JC, Voisin N, Andreadis KM, Pappenberger F, Phanthuwongpakdee N, Hall AC, Bates PD (2013) A first large-scale flood inundation forecasting model. Water Resour Res 49(10):6248-6257. doi:10.1002/wrcr.20521

Schumann GJP, Bates PD, Neal JC, Andreadis KM (2014) Fight floods on a global scale. Nature 507(7491):169

Shiklomanov AI, Lammers RB (2009) Record Russian river discharge in 2007 and the limits of analysis. Environ Res Lett 4(4):045015. doi:10.1088/1748-9326/4/4/045015

Skøien JO, Blöschl G, Western AW (2003) Characteristic space scales and timescales in hydrology. Water Resour Res 39(10):1304. doi:10.1029/2002WR001736

Smith LC (1997) Satellite remote sensing of river inundated area, stage, and discharge: a review. Hydrol Process 11: 1427-1439.

Smith LC, Pavelsky TM (2008) Estimation of river discharge, propagation speed, and hydraulic geometry from space: Lena River, Siberia. Water Resour Res 44: W03427. doi:10.1029/2008GL033268

Smith LC, Pavelsky TM (2009) Remote sensing of volumetric storage change in lakes. Earth Surf Process Landf 34:1353-1358.

Smith LC, Isacks BL, Forster RR, Bloom AL, Preuss I (1995) Estimation of discharge from braided glacial rivers using ERS-1 SAR: First results. Water Resour Res 31(5): 1325-1329.

Smith LC, Isacks BL, Bloom AL, Murray AB (1996) Estimation of discharge from three braided rivers using synthetic aperture radar (SAR) satellite imagery: Potential application to ungaged basins. Water Resour Res 32(7): 2021-2034.

Smith LC, Sheng Y, MacDonald GM, Hinzman LD (2005) Disappearing Arctic lakes. Science 308(5727):1429. doi:10.1126/science.1108142

Steunou N, Desjonquères JD, Picot N, Sengenes P, Noubel J, Poisson JC (2015) AltiKa altimeter: instrument description and in flight performance. Marine Geodesy (in press)

Verdin KL, Greenlee SK (1998) HYDRO1k documentation, US Geological Survey. https://lta.cr.usgs.gov/HYDRO1KReadMe. Accessed 24 February 2015.

Verpoorter C, Kutser T, Seekell DA, Tranvik LJ (2014) A global inventory of lakes based on high resolution satellite imagery. Geophys Res Lett 41(18):6396-6402. doi:10.1002/2014GL060641

Walter KM, Smith LC, Chapin FS (2007) Methane bubbling from northern lakes: present and future contributions to the global methane budget. Philos Trans Royal Soc A-Math Phys Eng Sci 365(1856):1657-1676. doi:10.1098/rsta.2007.2036

Wolf AT, Natharius JA, Danielson JJ, Ward BS, Pender JK (1999) International river basins of the world. Int J Water Resour Dev 15(4):387-427

Wood EF, Roundy JK, Troy TJ, van Beek LPH, Bierkens MFP, Blyth E, de Roo A, Döll P, Ek M, Famiglietti J, Gochis D, van de Giesen N, Houser P, Jaffé PR, Kollet S, Lehner B, Lettenmaier DP, Peters-Lidard C, Sivapalan M, Sheffield J, Wade A, Whitehead P (2011) Hyperresolution global land surface modeling: Meeting a grand challenge for monitoring Earth's terrestrial water. Water Resour Res 47(5):W05301. doi:10.1029/2010WR010090

Yamazaki D, Kanae S., Kim H, Oki T (2011) A physically based description of floodplain inundation dynamics in a global river routing model. Water Resour Res, 47(4): W04501. doi:10.1029/2010WR009726

Yoon Y, Durand MT, Merry CJ, Clark EA, Andreadis KM, Alsdorf DE (2012) Estimating river bathymetry from data assimilation of synthetic SWOT measurements. J Hydrol 464:363–375. doi:10.1016/j.jhydrol.2012.07.028

Yoon Y., Durand, MT, Merry CJ, Rodríguez E (2013) Improving Temporal Coverage of the SWOT Mission Using Spatiotemporal Kriging. IEEE IEEE J Sel Top Appl Earth Obs Remote Sens 6(3):1719-1729. doi:10.1109/JSTARS.2013.2257697

Zhang S, Gao H, Naz BS (2014) Monitoring storage in South Asia from multisatellite remote sensing. Water Resour Res 50(11):8927-8943. doi:10.1002/2014WR015829

Zhou T, Nijssen B, Gao H, Lettenmaier DP (in review) The contribution of reservoirs to global land

surface water storage variations. Submitted to J Hydrometeorol

Table 1 SWOT mission science requirements and goals (Rodríguez 2015)

Observed areas	- All observed water area will be provided - Errors are *evaluated* for (250 m)^2 (= 62 500 m^2) water bodies and 100 m (width) x 10 km (long) river reaches - Error are *characterized* for (100 m)^2 to (250 m)^2 water bodies and 50 m to 100 m (width) x 10 km (long) river reaches
Height accuracy	< 10 cm when averaging over water area > 1 km^2 < 25 cm when averaging over (250 m)^2 < water area < 1 km^2
Slope accuracy	1.7 cm/km for evaluated river reaches when averaging over water area > 1 km^2
Relative error on water areas	<15% for evaluated water body and river reaches < 25% of total characterized water body and river reaches
Mission lifetime	3 months of fast sampling calibration orbit + 3 years of nominal orbit
Rain/Layover/Frozen water flag	68%
Data collection	> 90% of all ocean/continents within the orbit during 90% of operational time

Table 2 SWOT mission characteristics

Orbit	Altitude	890 km
	Inclination	77.6°
	Repeat period	20.86 days
KaRIn (core payload)	One swath extent (total swaths: 2)	50 km
	Distance between the 2 swaths outer edges	120 km
	Distance between the 2 swaths inner edges (“nadir gap”)	20 km
	Radar frequency/wavelength	35.75 GHz/8.6 mm (Ka-band)
	Distance between the 2 antennas (baseline)	10 m
	Instrument azimuth pixel size (radar projection)	6 to 7 m
	Instrument range pixel size (radar projection)	From 60 m (near range, incidence angle ~0.6°) to 10 m (far range, ~3.9°)
Additional science payload	Nadir altimeter	Similar to the dual frequency (Ku/C) Poseidon-3 nadir altimeter on Jason-2
	Precise orbit determination system	- Laser retroreflector - DORIS receiver - GPS receiver
	Radiometer (usable only over oceans)	3-frequency (18, 23, 34 GHz) radiometer, similar to Advanced Microwave Radiometer on Jason-2

Table 3 Current discharge algorithms designed to use SWOT data (*n* means Manning coefficient, *w* river width, *S* river surface slope, *H* river elevation, A_0 unobserved cross-sectional flow area and *Q* discharge)

Discharge algorithm	Algorithm Basis	Tested river types	SWOT variables used	1st guess/ ancillary data	Output(s)
AMHG (Gleason and Smith 2014; Gleason et al. 2014)	*w*/*Q* geomorphic scaling relationship along river reach	Single channel & width variability & no lateral in/outflows & no several order magnitude variation & b>0.1 (in $w=aQ^b$)	*w*	-	*Q*
B2007 (Bjerklie et al. 2003, Bjerklie et al. 2005, Bjerklie 2007)	Manning-like equation with calibrated exponent and time varying Manning coefficient	Single channel	*H*, *w*, constant *S*	Mean annual *n* and *Q*	*Q*, time varying *n*
GM2015 (Garambois and Monnier, 2015)	Shallow water equations (low Froude)	Single channel & no in/outflows	δH, *w*, *S*	*n*, A_0, baseflow *Q*	*Q*, corrected *n*, corrected A_0
MetroMan (Durand et al. 2014)	Diffusive approximation of shallow water equations	Single channel	δH, *w*, *S*	*n*, A_0, baseflow *Q*	*Q*, corrected *n*, corrected A_0

Table 4 Published SWOT-related studies using data assimilation (DA) or optimal interpolation (OI) to correct/optimize different variables (*d* means water depth, *H* water elevation, *w* width, *S* water surface slope, *Q* discharge, A_i inundation area, *Z* bathymetric elevation, S_z bathymetric slope, *n* Manning coefficient). In this table, (L)EnKF/S stands for *(Local) Ensemble Kalman Filter/Smoother*, LSTOK for *Local Space-Time Ordinary Kriging*, LEnTKF for *Local Ensemble Transform Kalman Filter*, EKF for *Extended Kalman Filter*, RK for *River Kriging* and MPC for *Model Predictive Control*

Reference	DA/OI schemes	Model(s) + error	SWOT obs used + error	Corrected/ optimized variable(s)/ parameter(s)	Study domain
Andreadis et al. (2007)	EnKF	Hyrodynamic model + inflows errors	*d* (140km swath, 8-day/16-d/32-d orbit) + white noise	*d*	Ohio River (50km reach)
Durand et al. (2008)	EnKF	Hydrodynamic model + S_z and *n* errors	*H* (140km swath, 16-day orbit) + white noise	*Z*, S_z	Amazon River (240km reach)
Biancamaria et al. (2011)	LEnKF+ LEnKS	Hydrodynamic model + precip errors	*d* (140km swath, 22-day orbit) + white noise	*d*	Ob River (1120km)
Yoon et al. (2012)	EnKF+ LEnKS	Hydrodynamic model + precip errors/*z* errors/*z* spatial auto-correlation	*H*, *S*, *w* (140km swath, 22-day orbit) + white noise	*Z*, *d*	Ohio basin river system
Yoon et al. (2013)	LSTOK	-	*d* (140km swath, 22-d orbit) + white noise	*d* at times with no SWOT obs	Tennessee River (1050km)
Andreadis and Schumann (2014)	LEnTKF	Hydrodynamic model + sampling historical simulation	*H*, *w*, A_i (multi sat missions) + white noise	Initial condition to forecast model	Ohio River (500km reach)
Pedinotti et al. (2014)	EKF	Hydrologic model (0.5°×0.5° pixels) + *n* errors	*d* (140km swath, 22-d orbit) + white noise	*n*	Whole Niger basin
Paiva et al. (2015)	RK	Space-time *Q* covariance from diffusive wave approx. St-Venant eq	*d*, *S*, *w*, *Q* (140km swath, 22-day orbit) + white noise	*Q* at times with no SWOT obs	Ganges-Brahmaputra-Meghna river system in Bangladesh
Munier et al. (2015)	LEnKS + MPC	Hydrodynamic model & reservoir model + precip errors	*d* (120km swath, 21-d orbit) + white noise	*d* + optimized reservoir release	Upper Niger basin and Selingue reservoir

1230 **Table 5** Published SWOT-related studies on lakes and reservoirs

Reference	Method	SWOT obs.	Study domain
Biancamaria et al. (2010)	Parametrization of global annual storage variation	Lakes area > $(250m)^2$ and height variations> SWOT height accuracy	Extrapolation of global lakes distribution
Lee et al. (2010)	Lake storage change from optical image, satellite altimetry, *in situ* gage and parametrization	δH with white noise function of lake area (140km swath, 3-day and 22-day orbit)	Multiple Arctic lakes
Munier et al. (2015)	Hydrologic model, hydrodynamic model + DA of SWOT obs., reservoir model + release optimization	d (120km swath, 21-day orbit) + white noise	Upper Niger basin and Selingue reservoir

1231

Fig. 1 Time-space diagrams of continental water surface processes and SWOT observation window. Inspired from Blöschl and Sivapalan (1995) and Skøien et al (2003)

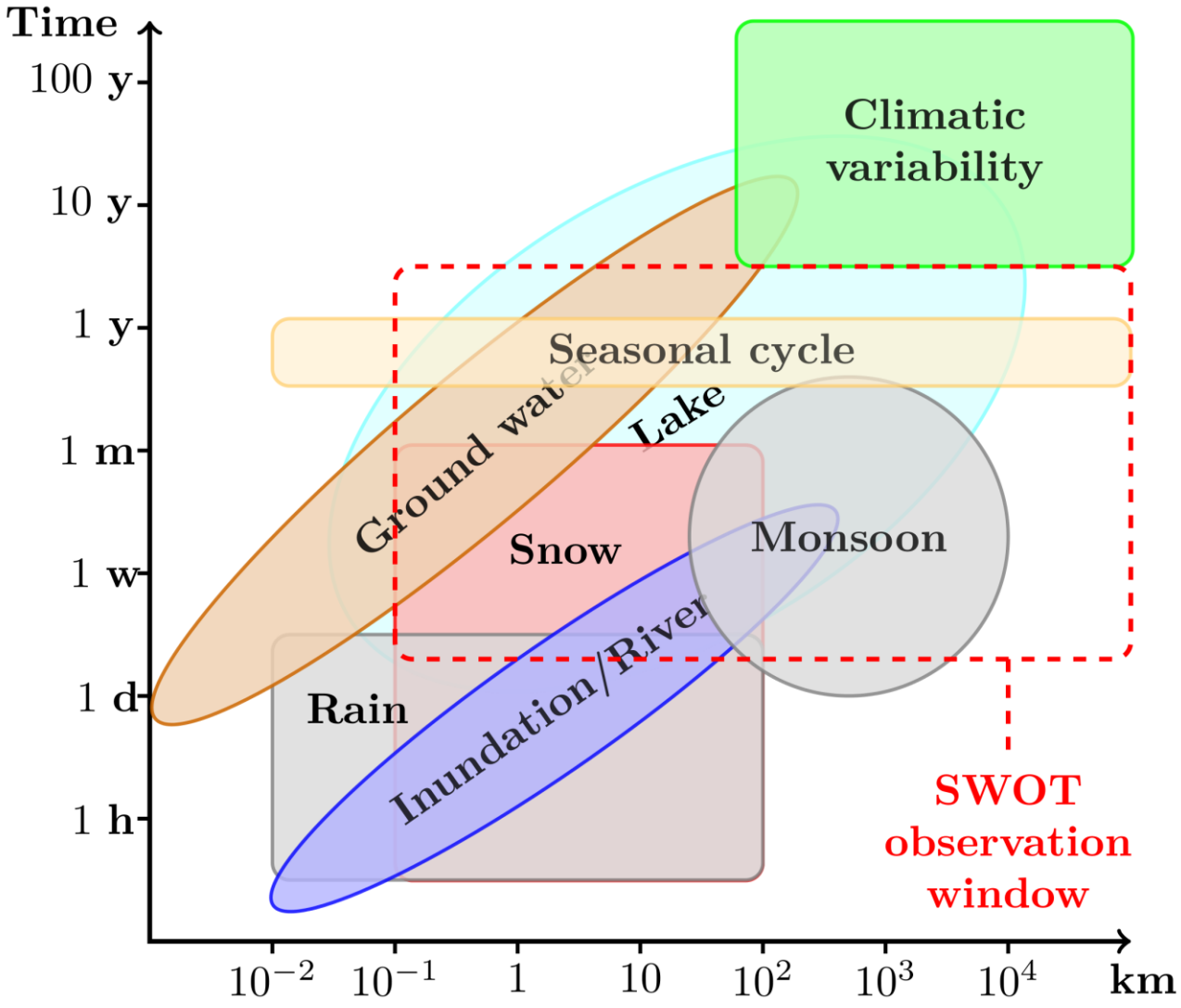

Fig. 2 Conceptual view of the future SWOT mission with its principal payloads: the Ka-band Radar Interferometer (KaRIn, with the observed swaths shown by the yellow polygons) and a Ku-band nadir altimeter (yellow line). Satellite size and altitude are not to scale compared to the Google Earth background image (South West of France), but the ground swaths are (background image: Google earth, Landsat image, data SIO, NOAA, U.S. Navy, NGA, GEBCO)

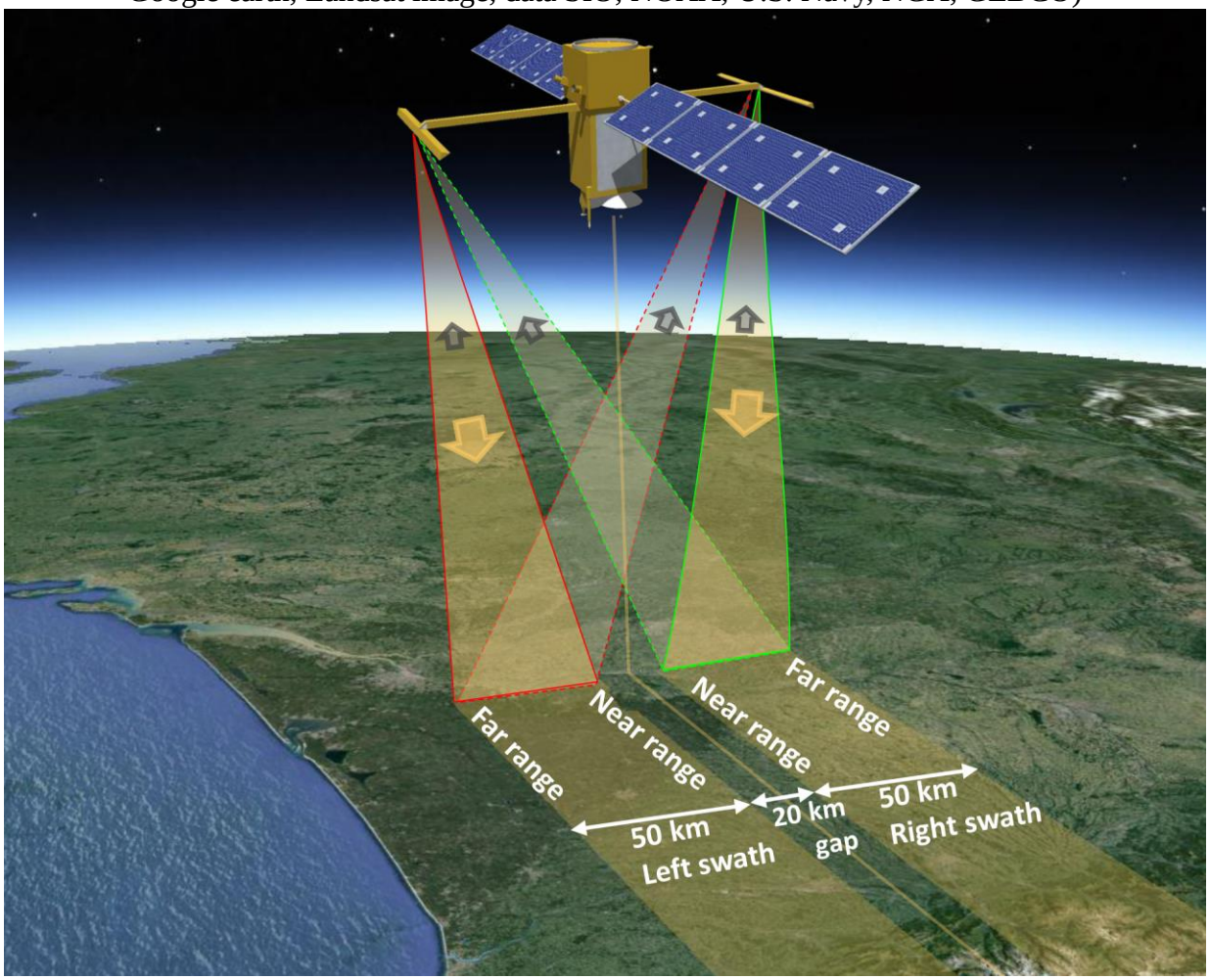

Fig. 3 Number of SWOT revisits per orbit repeat period (21 days) over the continents (ocean have been masked, but ocean data will also be provided) in between 78°S and 78°N (a.) and a zoom over the Lower Amazon (b.). Over the Lower Amazon, white diamonds with magenta boundaries corresponds to observation gaps due to the orbit intertrack distance

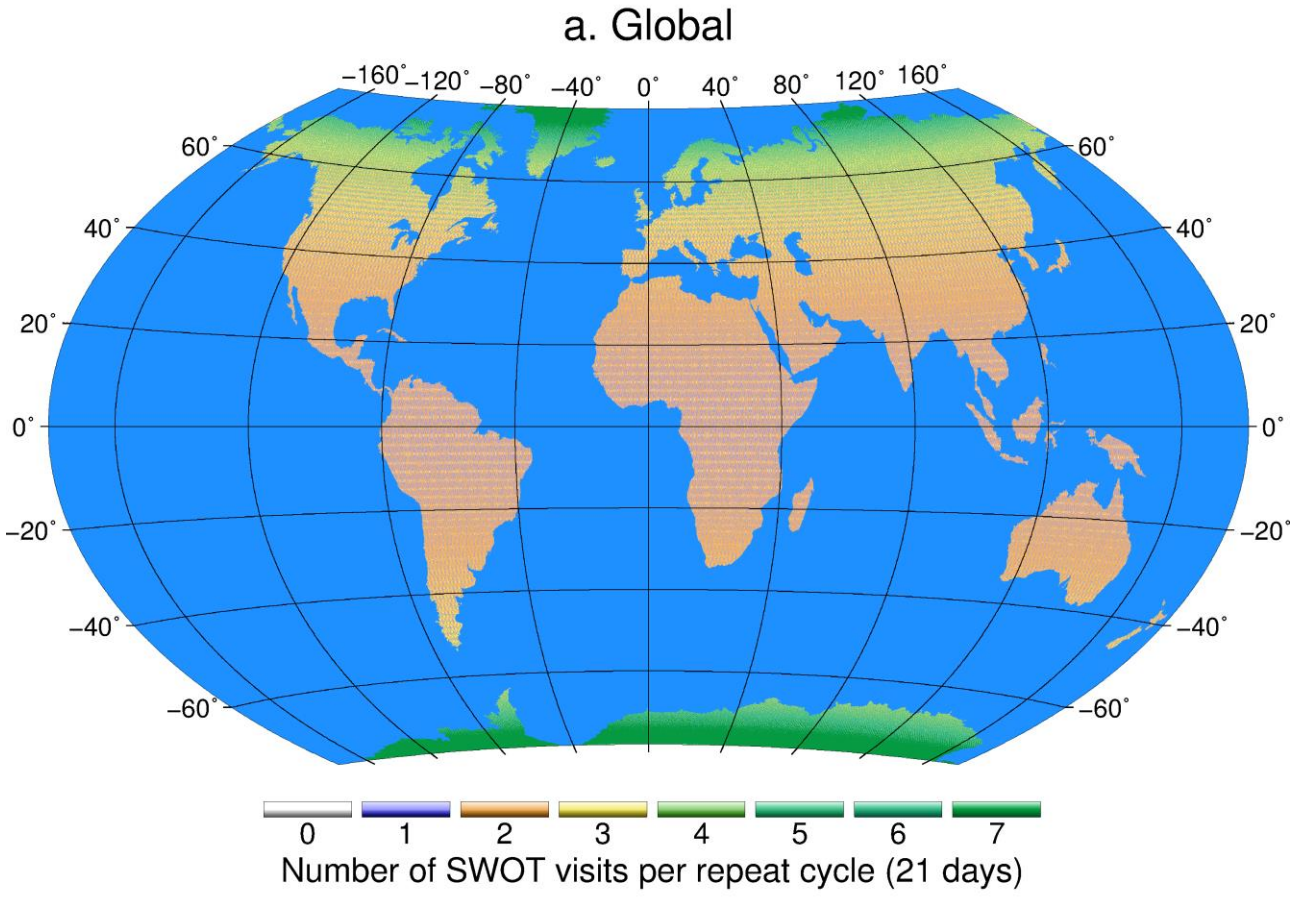
a. Global
−160°
−120°
−80°
−40°
0°
40°
80°
120°
160°
60°
40°
20°
0°
−20°
−40°
−60°
0
1
2
3
4
5
6
7
Number of SWOT visits per repeat cycle (21 days)

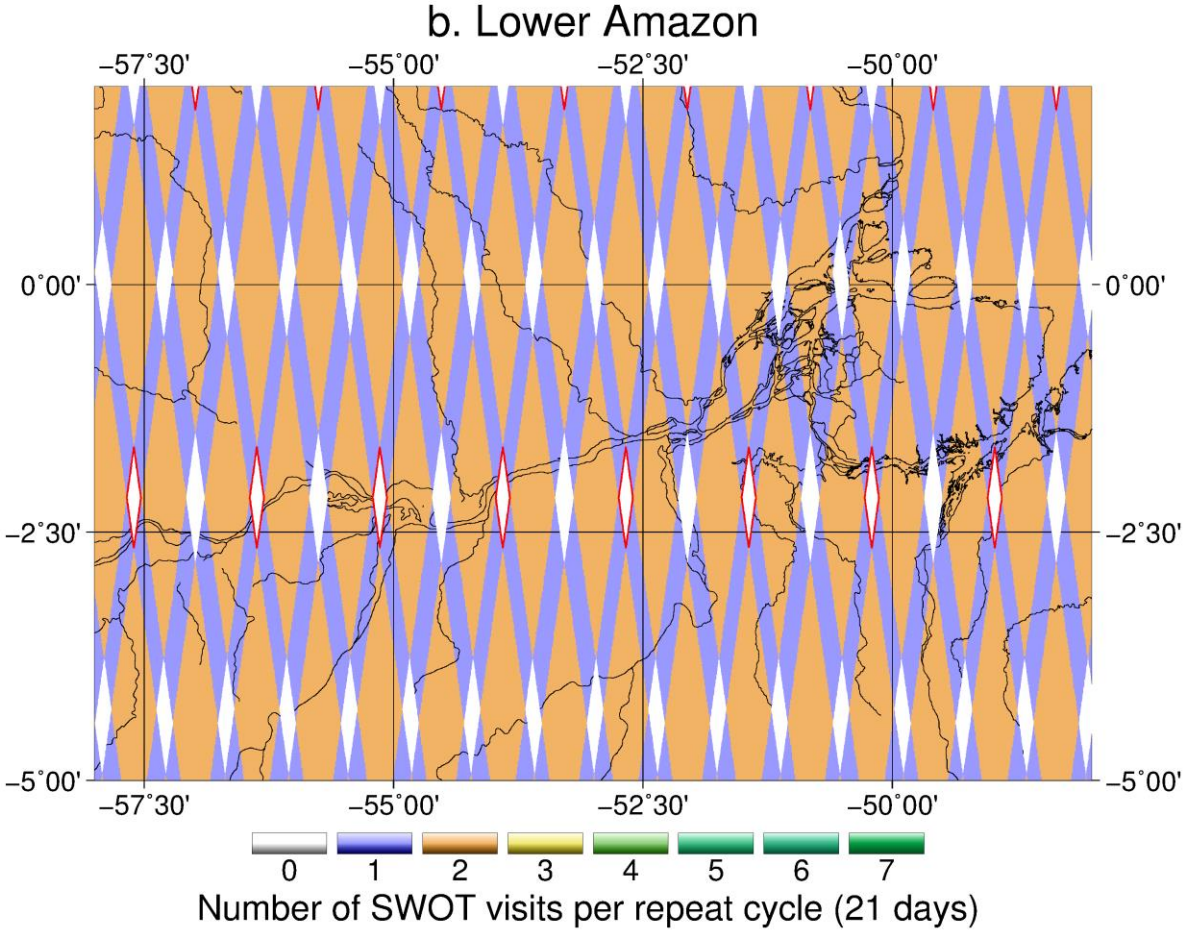
b. Lower Amazon
−57°30'
−55°00'
−52°30'
−50°00'
0°00'
−2°30'
−5°00'
0
1
2
3
4
5
6
7
Number of SWOT visits per repeat cycle (21 days)

1251
1252

Fig. 4 SWOT observations mask (black bars correspond to an observation) along 30°E meridian versus days (during an orbit repeat period)

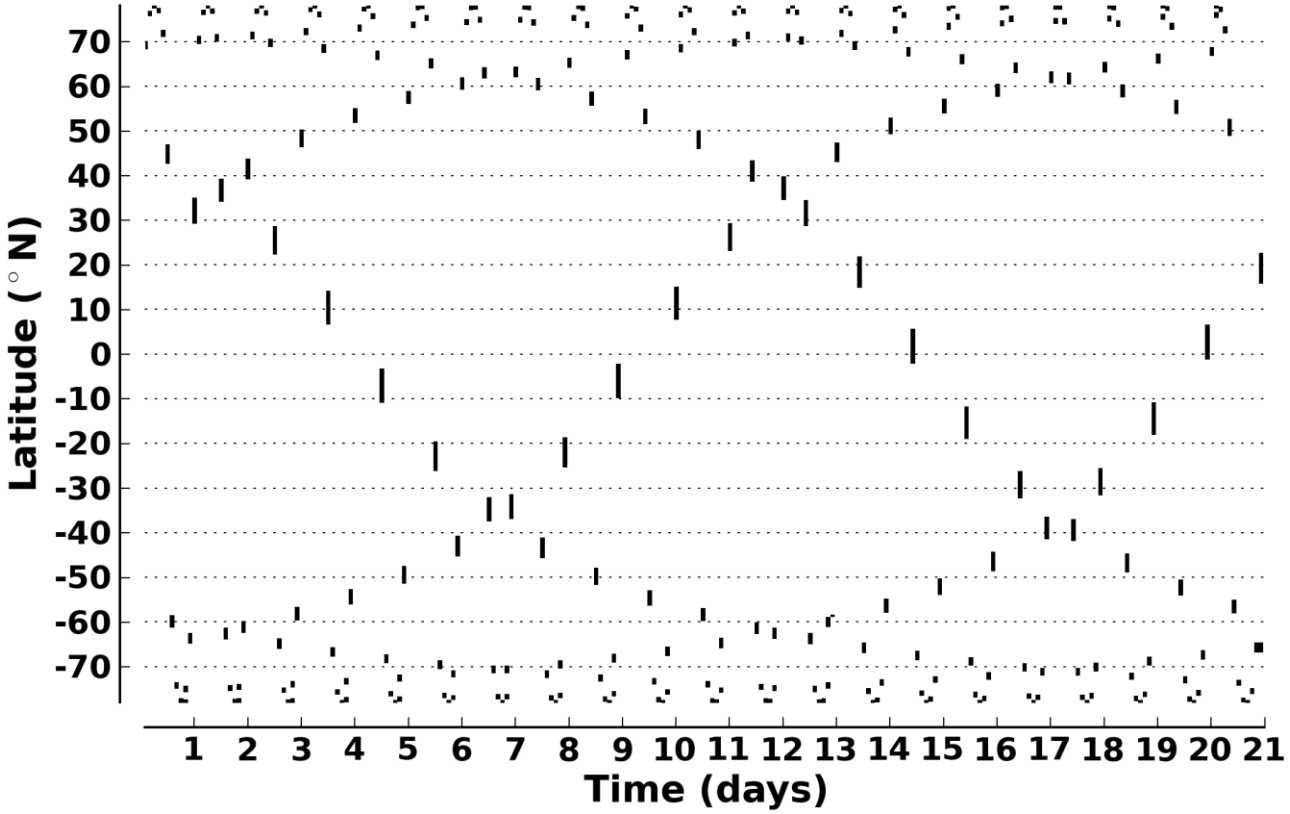

Fig. 5 Conceptual sketches of SWOT Observing System Simulation Experiments (OSSE) using optimal interpolation (a.) or data assimilation (b.)

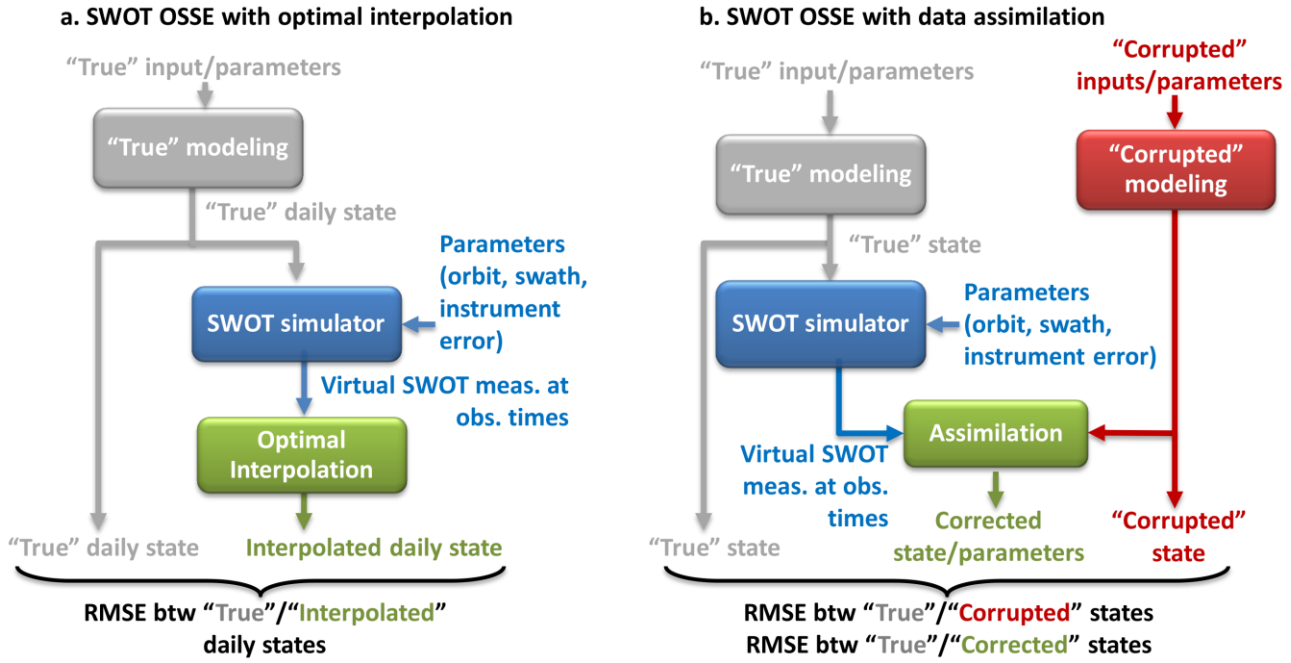

Fig. 6 Cumulative lake storage change (in % of the total lake storage change of the ensemble mean) versus lake area for 100 realizations of the log-normal random distribution of the annual water level variation estimated by Biancamaria et al. 2010. The ensemble mean corresponds to the green curve